Potentiation of Gram-positive specific antibiotics against Gram-negative bacteria through outer membrane disruption

Wesseling, C.M.J.

Chapter 3

Thrombin-derived peptides potentiate the activity of Gram-positive specific antibiotics against Gram-negative bacteria

Charlotte M. J. Wesseling,[‡] Thomas M. Wood,[‡] Cornelis J. Slingerland, Kristine Bertheussen, Samantha Lok, and Nathaniel I. Martin

[‡]*These authors contributed equally to this work*

Parts of this chapter have been published: *Molecules*. **2021**, 26 (7), 1954.

Abstract

The continued rise of antibiotic resistance threatens to undermine the utility of the world's current antibiotic arsenal. This problem is particularly troubling when it comes to Gram-negative pathogens for which there are inherently fewer antibiotics available. To address this challenge, recent attention has been focused on finding compounds capable of disrupting the Gram-negative outer membrane as a means of potentiating otherwise Gram-positive-specific antibiotics. In this regard, agents capable of binding to the lipopolysaccharide (LPS) present in the Gram-negative outer membrane are of particular interest as synergists. Recently, thrombin-derived C-terminal peptides (TCPs) were reported to exhibit unique LPS-binding properties. We here describe investigations establishing the capacity of TCPs to act as synergists with the antibiotics erythromycin, rifampicin, novobiocin, and vancomycin against multiple Gram-negative strains including polymyxin-resistant clinical isolates. We further assessed the structural features most important for the observed synergy and characterized the outer membrane permeabilizing activity of the most potent synergists. Our investigations highlight the potential for such peptides in expanding the therapeutic range of antibiotics typically only used to treat Gram-positive infections.

1. Introduction

The rising tide of antibiotic resistance presents a clear threat to global health. This threat, coupled with the well-documented dearth of new antibiotics in the development pipeline, means that resistant pathogens are even more problematic.[1] Based on current trends, the World Health Organization (WHO) predicts that infections due to resistant bacteria will be the leading cause of death globally by 2050.[2] The WHO recently published its updated "pathogen threat list" of which three drug-resistant Gram-negative species were assigned top priority: carbapenem-resistant *Acinetobacter baumannii*, *Pseudomonas aeruginosa*, and *Enterobacteriaceae*.[3] The emergence and proliferation of such resistant Gram-negative pathogens is concerning given the limited number of viable treatment options available.[3]

It is well established that compared to Gram-positive pathogens, Gram-negative bacteria are more difficult to kill with antibiotics due to the presence of an additional barrier: the outer membrane (OM).[4,5] The OM protects Gram-negative bacteria from a large number of antibiotics that are used clinically to treat infections with Gram-positive bacteria.[4] Disruption of the OM has been widely investigated and in some cases proven to be an effective method to enable such antibiotics to function against Gram-negative bacteria.[6–10] In this regard, combinations of a membrane disruptor such as the well-studied polymyxin B nonapeptide (PMBN, Figure 1) along with macrolides or rifamycin-type antibiotics represent classic examples of such synergistic activity: the use of a combination leads to better results than a sum of each of the separate components.[6,7,11–14] Notably, the polymyxin derivative SPR741 (Figure 1), a selective OM disruptor developed by Spero Therapeutics, recently passed Phase I clinical trials.[13,15,16]

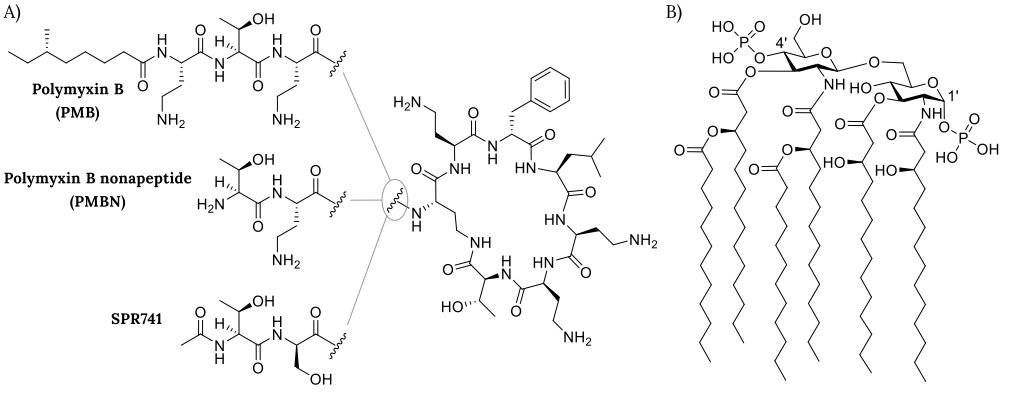

Figure 1. Structures of: A) polymyxin B (PMB), polymyxin B nonapeptide (PMBN), and SPR741; B) Lipid A component of the Gram-negative lipopolysaccharide (LPS).

Like its parent polymyxin B (Figure 1), SPR741 targets the bacterial lipopolysaccharide (LPS), a major component on the OM outer leaflet.[4,14,17] The core of LPS consists of Lipid A, a heavily lipidated disaccharide bearing phosphate groups at the 1' and

4' positions (Figure 1).[4] Small cations such as Mg^{2+} and Ca^{2+} bridge the negative charges of the phosphate groups and in doing so contribute to the tight packing of LPS.[4,6] It is generally held that highly positively charged compounds such as PMBN bind the negatively charged LPS with high affinity and in doing so interfere with LPS packing, leading to OM permeabilization.[7,18–21]

Compounds that bind to LPS with high affinity are also often referred to as endotoxin neutralizing compounds. Such compounds can demonstrate beneficial effects in reducing the inflammatory responses associated with systemic LPS exposure as in the case of sepsis.[22–25] In recent years, an increasing number of reports have appeared describing the synergistic effects of various positively charged small molecules and peptide-based compounds that interact with LPS.[24–33]

Given the apparent link between LPS binding, OM permeabilization, and antibiotic potentiation, we set out to identify literature compounds described as having affinity for LPS that had not yet been evaluated for synergy with Gram-positive specific antibiotics. This led us to the family of thrombin-derived C-terminal peptides (TCPs) reported by Schmidtchen and coworkers. In 2010, the Schmidtchen group first reported that peptide fragments from the C-terminus of thrombin, a key enzyme in the coagulation cascade, exhibit activity as host-defense peptides.[34] Subsequent structure activity studies by the same group identified peptide sequences with optimal antibacterial activity and recent NMR studies have elucidated the structural basis for their interaction with LPS.[26,35,36]

In the present study we set out to assess the potential for TCPs to potentiate the anti-Gram-negative activity of otherwise inactive Gram-positive specific antibiotics. To do so, synergy assays were first conducted using the TCPs described in the literature in combination with various antibiotics. Our initial studies revealed that, as we had hypothesized, the TCPs do indeed exhibit synergy. Building from these results we then prepared a number of new peptide analogues to assess the structural elements most important for synergy. Notably, we found that synergistic activity does not necessarily directly correlate with the inherent antibacterial activity of these peptides. We here report several new peptides inspired by thrombin-derived C-terminal peptides that display enhanced synergistic effects and reduced hemolytic activity.

2. Results

2.1. Synergy with thrombin-derived C-terminal peptides

To begin, we selected four peptides previously described by the Schmidtchen group as LPS-binding.[26] The sequences of these peptides (**1–4**) are provided in Table 1 and range in length from 12 to 25 amino acids. Common to all four is the core sequence previously reported to be responsible for LPS binding.[26] The peptides were readily synthesized using solid-phase peptide synthesis (SPPS) and screened for synergistic activity using checkerboard assays. Synergy was initially assessed in combination with erythromycin (Figure 2, also see Supplementary data, Figure S1) and rifampicin (See Supplementary data, Figure S2) in Lysogeny Broth (LB) using *Escherichia coli* BW25113 as the indicator strain. Synergy is quantified by means of the fractional inhibitory concentration index (FICI) where an FICI of ≤0.5 is defined as synergistic and the lower the value, the more synergistic the combination.[37]

Prior to assessing synergy, the minimum inhibitory concentrations (MICs) of the peptides themselves were measured revealing that they exhibit little-to-no inherent activity with MICs equal to, or above, the maximum 200 μg/mL concentration tested. The MICs of the companion antibiotics erythromycin and rifampicin were measured to be 100–200 μg/mL and 8 μg/mL, respectively (see Supplementary data, Tables S1 and S2). Using these parameters checkerboard assays were performed as illustrated in Figure 2. The results of the checkerboard assays performed with peptides **1–4** reveal clear differences in their synergistic potential. While the shortest peptide **1** exhibits potent synergy with erythromycin, the longer peptides **2–4** demonstrate comparatively little or no synergy (Table 1). In combination with rifampicin, peptides **1–4** all showed some synergistic activity with FICIs ranging from 0.094 to 0.313, but with peptide **1** again displaying the most potent synergy (see Supplementary data, Table S2). These preliminary findings served to validate our hypothesis that LPS-binding peptides derived from thrombin have the capacity to synergize with Gram-positive specific antibiotics. All peptides were also screened for hemolytic activity which revealed a clear trend: while the shorter peptides **1** and **2** showed no appreciable hemolytic activity, the longer peptide **3** and **4** were highly hemolytic (Table 1). This hemolysis data, combined with the synergistic activity observed, led us to select peptide **1** for further investigation.

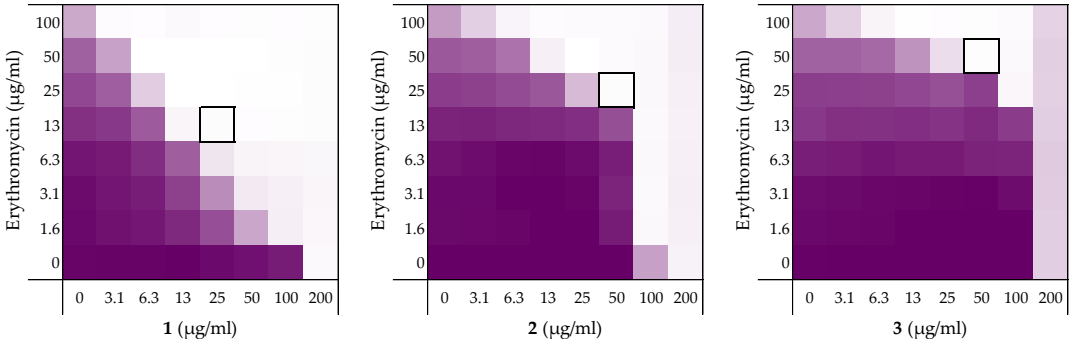

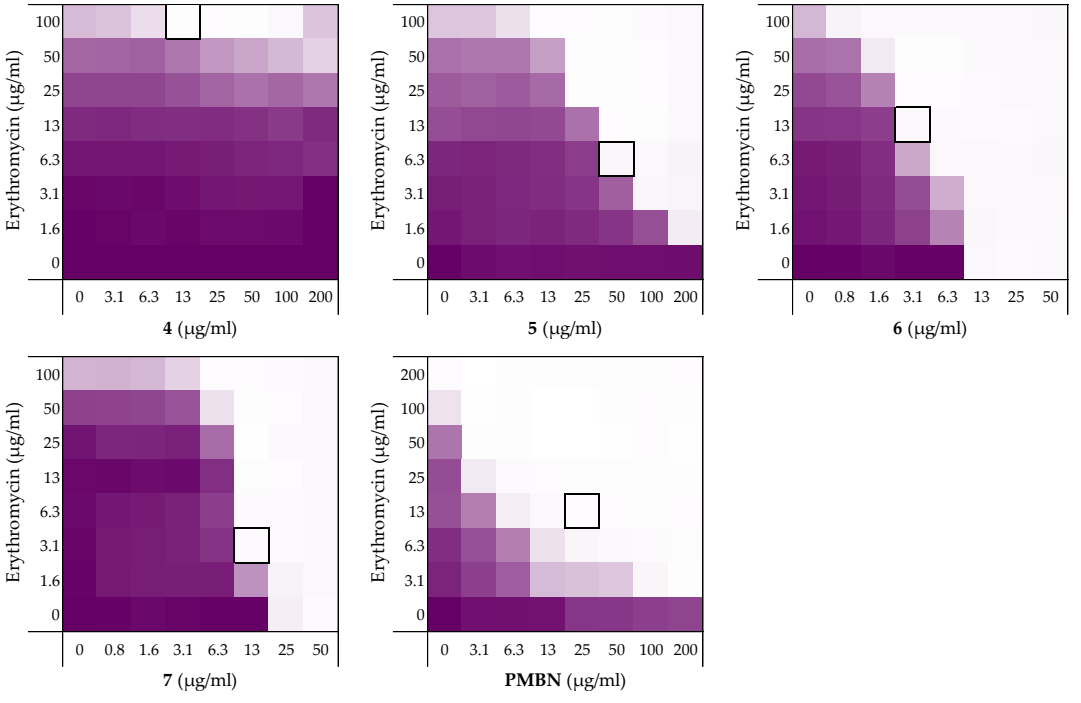

Figure 2. Checkerboard assays of the peptides **1**-**7** and PMBN in combination with erythromycin versus *E. coli* BW25113. In each case the bounded box in the checkerboard assays indicates the combination of peptide and antibiotic resulting in the lowest FICI (see Table 1). OD_{600} values were measured using a plate reader and transformed to a gradient: purple represents growth, white represents no growth. An overview of all checkerboard assays with erythromycin can be found in the Supplementary data, Figure S1.

Table 1. Overview of the TCPs peptide sequence, synergistic and hemolytic activity.

	Peptide sequence	MIC	$MSC_{peptide}$	FICI	Hemolysis[b]
1	H_2N-VFRLKKWIQKVI-OH	200	25	0.188	0%
2	H_2N-HVFRLKKWIQKVIDQFGE-OH	200	50	0.375	9%
3	H_2N-FYTHVFRLKKWIQKVIDQFGE-OH	200	50	0.500	43%
4	H_2N-GKYGFYTHVFRLKKWIQKVIDQFGE-OH	>200	12.5	>0.5[a]	70%
5	Ac-VFRLKKWIQKVI-OH	>200	50	0.156	0%
6	H_2N-VFRLKKWIQKVI-NH_2	12.5	3.13	0.313	4%
7	Ac-VFRLKKWIQKVI-NH_2	50	12.5	0.266	5%
PMBN		>200	25	0.125	-

[a]Synergy defined as an FICI ≤0.5[37]; [b]Hemolysis was determined after a 20 hour incubation of the compounds (200 μg/ml) with defibrinated sheep blood (see Supplementary data, Figure S4 and Table S4).

Building on these findings and with peptide **1** as our lead synergist, we next explored the impact of changes to the N- and C-termini of the peptide. To this end,

peptides **5–7** were prepared to examine the impact of N-terminal acetylation and/or C-terminal amidation. N-terminal acetylation alone as in peptide **5** was found to have minimal effect on the inherent activity or synergistic potential of the peptide. By comparison, C-terminal amidation as in peptides **6** and **7** led to a significant increase in the inherent antibacterial activity with little impact on hemolytic activity. The reduced MIC values thus achieved, particularly notable for peptide **6**, provides a key advantage in that a lower concentration of peptide is required to achieve synergy: peptide **6** has an minimum synergistic concentration (MSC) of 3.125 μg/mL versus 25 μg/mL of its parent peptide **1** (Table 1). To assess whether peptide **6** employs an LPS mediated mechanism of action similar to peptide **1**, an LPS competition assay was also performed. Notably, the MIC of peptide **6** was found to increase from 12.5 μg/mL to 200 μg/mL in the presence of 1 mg/mL of LPS (See Supplementary data, Figure S4 and Table S4). This finding indicates that the antimicrobial activity of peptide **6** relies on LPS binding. Based on its enhanced activity and confirmed LPS-dependent mechanism, we next took peptide **6** forward for additional structure-activity studies by means of an alanine scan.

2.2. Alanine scan of peptide 6

To assess the role of the individual amino acids in peptide **6** and their specific contribution to both the inherent activity and synergistic activity of the peptide, an alanine scan was performed. Like the parent peptide, peptides **8–19** (Table 2) were synthesized as the C-terminus amides using microwave-assisted automated SPPS. As summarized in Table 2, the MICs of the alanine scan peptides ranged from 12.5 μg/mL, as for peptide **6**, to above the maximum concentration tested of 200 μg/mL. After establishing the individual MICs for peptides **8–19**, checkerboard assays were performed as shown in Figure 3. The FICI values thus obtained clearly show that the alanine exchange introduced in peptides **12**, **13**, and **17** leads to a complete loss of synergistic activity. Notably, the common feature in these three peptides is the replacement of a lysine residue with alanine. Moreover, while no longer synergistic with erythromycin, these peptides still have a relatively low MIC of 25 μg/mL. Hemolysis data offers insight into this trend: the KΔA peptides **12**, **13**, and **17** are all hemolytic, which suggests a nonselective membrane disruption mode of action. By comparison, none of the other alanine scan peptides show appreciable hemolytic activity (Table 2).

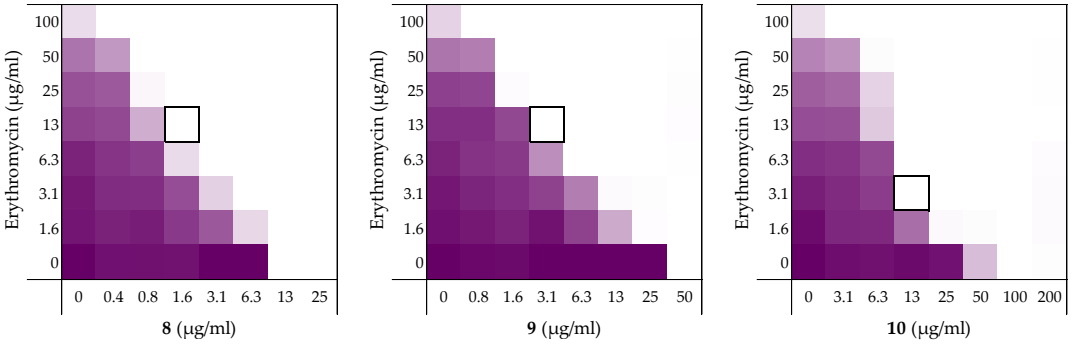

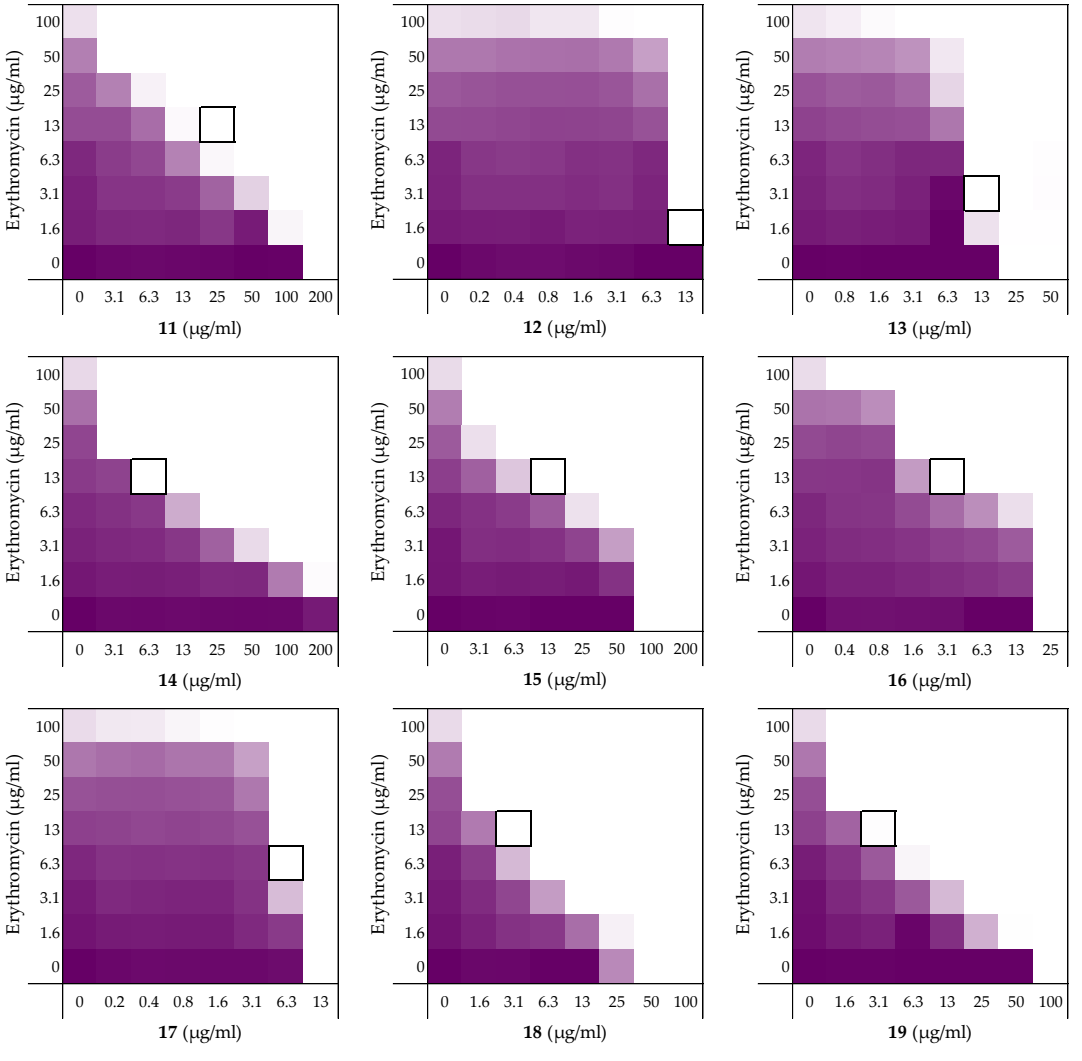

Figure 3. Checkerboard assays of the Ala-scan peptides **8**-**19** in combination with erythromycin versus *E. coli* BW25113. In each case the bounded box in the checkerboard assays indicates the combination of peptide and antibiotic resulting in the lowest FICI (see Table 2). OD_{600} values were measured using a plate reader and transformed to a gradient: purple represents growth, white represents no growth. An overview of all checkerboard assays with erythromycin can be found in the Supplementary data, Figure S1.

Somewhat surprisingly, all of the other peptides prepared in the alanine scan study were found to exhibit more potent synergistic activity than peptide **6**. Notably, these peptides all exhibit synergy at concentrations lower than required for PMBN (see Table 1 and Table 2). In addition, an apparent trend emerges from the alanine scan data where decreased antimicrobial activity is inversely proportional to the synergistic activity of the peptides.

Table 2. Overview of the Ala-scan peptide sequences, antimicrobial, synergistic and hemolytic activity. MIC and FICI values were obtained from the checkerboard assay shown in Figure 3.

	Peptide sequence	MIC[a]	FICI	Hemolysis[c]
6	H_2N-VFRLKKWIQKVI-NH_2	12.5	0.313	4%
8	H_2N-**A**FRLKKWIQKVI-NH_2	12.5	0.188	2%
9	H_2N-V**A**RLKKWIQKVI-NH_2	50	0.125	0%
10	H_2N-VF**A**LKKWIQKVI-NH_2	100	0.141	4%
11	H_2N-VFR**A**KKWIQKVI-NH_2	200	0.188	1%
12	H_2N-VFRL**A**KWIQKVI-NH_2	25	>0.5[b]	30%
13	H_2N-VFRLK**A**WIQKVI-NH_2	25	>0.5[b]	19%
14	H_2N-VFRLKK**A**IQKVI-NH_2	>200	0.078	1%
15	H_2N-VFRLKKW**A**QKVI-NH_2	100	0.188	1%
16	H_2N-VFRLKKWI**A**KVI-NH_2	25	0.188	4%
17	H_2N-VFRLKKWIQ**A**VI-NH_2	12.5	>0.5[b]	21%
18	H_2N-VFRLKKWIQK**A**I-NH_2	50	0.125	2%
19	H_2N-VFRLKKWIQKV**A**-NH_2	100	0.094	1%

[a]MSC data can be found in Supplementary data, Table S1; [b]Synergy defined as an FICI ≤0.5[37]; [c]Hemolysis determined after a 20 hour incubation of the compounds (200 μg/ml) with defibrinated sheep blood. (see Supplementary data, Figure S4 and Table S4).

Among the non-hemolytic peptides generated in the alanine scan, only peptide **8** (V1ΔA) retains the same inherent antimicrobial activity as peptide **6** with an MIC of 12.5 μg/mL. It is, however, interesting to note that while replacement of other hydrophobic amino acids in peptide **6** with alanine as for **9**, **11**, **14**, **15**, **18**, and **19** did result in a decrease of antimicrobial activity, it also led to significant enhancement of synergistic activity (Table 2). Apparently, replacing the bulkier aromatic side-chains as in F2ΔA (**9**) and W7ΔA (**14**) is an especially favorable exchange when it comes to potentiating the activity of erythromycin. Notably, replacement of the C-terminal Ile residue as for I12ΔA (**19**) results in a strongly synergistic peptide, while replacing Ile in the center of the peptide as in I8ΔA (**15**) has a less profound effect. Moreover, while peptide **9** has the same FICI as PMBN (Table 1), peptides **14** and **19** are even more potent synergists.

As mentioned above, the cationic side-chains of the Lys residues present in peptide **6** are required for synergy and also serve to limit hemolysis. By comparison, alanine replacement of the polar but neutral glutamine, as in Q9ΔA (**16**), appears to have little effect. Moreover, the R3ΔA substitution in peptide **10**: the only other case wherein a positively charged side-chain was replaced by alanine, did not trigger hemolytic activity and retained synergistic activity. We therefore decided to also take peptide **10** along as part of a broader screening of the most potent synergistic peptides **14** and **19**.

2.3. Exploring the synergistic range

A well-studied example of synergy is the potentiation of erythromycin and rifampicin against Gram-negative bacteria by PMBN. Clinically, erythromycin and rifampicin are generally only used to treat infections due to Gram-positive pathogens as both exhibit rather limited activity against Gram-negative strains.[38–40] Other Gram-positive specific antibiotics, such as novobiocin and vancomycin, have also been shown to be capable of killing Gram-negative pathogens if combined with outer membrane disruptors.[10] To ascertain the potentiation range of peptides **6**, **10**, **14**, and **19** checkerboard assays with rifampicin, novobiocin, and vancomycin were performed. PMBN was also included to serve as a benchmark and to allow for comparison to other synergists described in literature.

In addition to investigating a broader panel of Gram-positive antibiotics, we were also curious to see how general the synergistic activity of peptides **6**, **10**, **14**, and **19** is against different Gram-negative pathogens. In the initial synergy assays performed the peptides were screened against the indicator strain *E. coli* BW25113. In the next phase of our study we selected a broader panel of Gram-negative bacteria selected from the WHO priority pathogen list. Specifically, we studied the capacity of peptides **6**, **10**, **14**, and **19** to enhance the activity of rifampicin against a range of *E. coli* strains including *mcr*-positive polymyxin-resistant isolates and strains of *A. baumannii*, *P. aeruginosa*, and *Klebsiella pneumoniae*.

2.3.1. Synergy with rifampicin, novobiocin, and vancomycin

As noted above (Section 2.1), the MIC of rifampicin against *E. coli* BW25113 was established to be 8 μg/mL. By comparison, novobiocin and vancomycin showed no antimicrobial activity against the same strain at concentrations as high as 200 μg/mL. However, when these antibiotics were combined with peptides **6**, **10**, **14**, and **19** a clear synergistic effect was observed in all cases. As noted above, peptides **14** and **19** demonstrated the most potent synergy when combined with erythromycin (Table 2). This effect was largely maintained when **14** and **19** were tested with rifampicin, novobiocin, and vancomycin (Figure 4 and Supplementary data Figures S5 and S6). Table 3 provides an overview of the FICI values obtained for peptides **6**, **10**, **14**, and **19** in combination with these antibiotics. In general, peptide **19** was found to be the most potent synergist and notably was found to be even more effective than PMBN in potentiating the activity of both novobiocin and vancomycin against the indicator strain.

Table 3. FICI values of peptides **6**, **10**, **14**, and **19** against *E. coli* BW25113 in combination with "Gram-positive-specific" antibiotics rifampicin, novobiocin, and vancomycin.[a]

Peptides	Rifampicin	Novobiocin	Vancomycin
6	0.156	0.188	0.188
10	0.141	0.078	0.156
14	0.141	0.031	0.250
19	0.078	0.039	0.078
PMBN	0.063	0.047	0.156

[a]MIC and MSC data can be found in the Supplementary data, Table S2, S5 and S6.

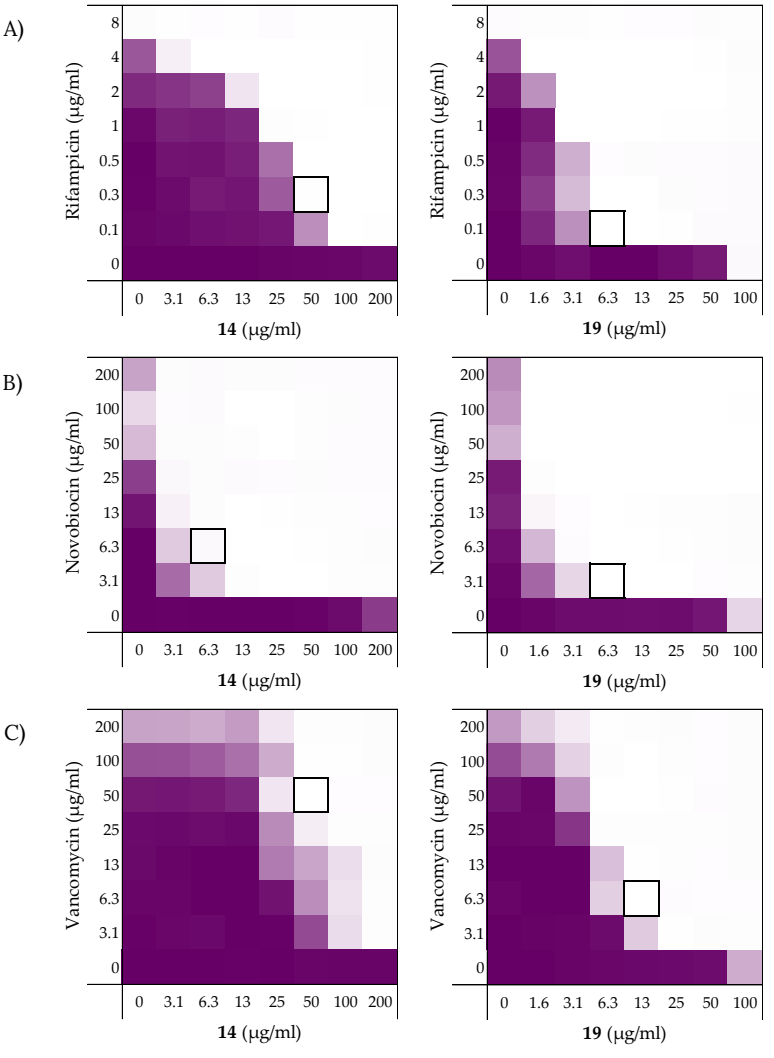

Figure 4. Checkerboard assays of the peptides **14** and **19** in combination with A) Rifampicin; B) Novobiocin; C) Vancomycin versus *E. coli* BW25113. In each case the bounded box in the checkerboard assays indicates the combination of peptide and antibiotic resulting in the lowest FICI (see Table 3). OD_{600} values were measured using a plate reader and transformed to a gradient: purple represents growth, white represents no growth. Checkerboard assays of peptide **6**, **10** and PMBN in combination with rifampicin, novobiocin and vancomycin are available in the Supplementary data, Figure S2, S5 and S6.

2.3.2. Synergy towards other *E. coli* strains including *mcr*-positive clinical isolates

Next, the synergistic activity of peptides **6**, **10**, **14**, and **19** in combination with rifampicin was tested against *E. coli* strains ATCC25922 and W3110. These strains were selected given that *E. coli* ATCC25922 has a smooth LPS layer, while *E. coli* W3110 lacks the O-antigen, giving it a rough LPS layer similar to *E. coli* BW25113.[41–43] The susceptibility of Gram-negative bacteria to antibiotics is known to be related to their LPS structure and we therefore set out to assess whether this might affect the efficacy of the synergists as well.[44] While the four peptides exhibited MICs of 200 μg/mL or above against the ATCC25922 strain (see Supplementary data, Table S7), all were found to be potent synergists (Table 4 and Figure 5A). Interestingly, the ATCC25922 strain was found to be more susceptible to these synergistic effects than the BW25113 indicator strain used in our initial screens (Table 4). The results obtained with the W3110 strain provided an interesting contrast: while peptides **6** and **10** exhibited some inherent antimicrobial activity, neither showed any ability to synergize with rifampicin (see Table 4 and Supplementary data, Table S8). Peptides **14** and **19**, however, exhibited potent synergistic activity in combination with rifampicin with peptide **19** resulting in FICI values equal-to or lower than those obtained with the *E. coli* BW25113 indicator strain.

To examine the impact of structurally modified LPS on the synergistic activity of peptides **6**, **10**, **14**, and **19**, the screening was continued with *E. coli* strains bearing *mcr*-1, *mcr*-2 and *mcr*-3 genotypes known to confer polymyxin resistance. Specifically, mcr-positive bacteria encode for a phosphoethanolamine transferase that modifies the structure of lipid A leading to a loss of activity for polymyxin antibiotics.[45,46] Synergy was confirmed for all *mcr*-positive strains with EQASmcr-1 and EQASmcr-3 shown to be most susceptible to synergy (Figure 5B,C, Table 4 and see Supplementary data, Tables S9–S12). Interestingly, potent synergy was observed for all four peptides with rifampicin indicating that the structurally modified LPS present in these strains does not interfere with the synergistic activity of peptides **6**, **10**, **14**, and **19**.

Table 4. FICI values of peptides **6**, **10**, **14** and **19** in combination with rifampicin against different *E. coli* strains including mcr-resistant strains.[a]

Pathogen	6	10	14	19
E. coli BW25113	0.156	0.141	0.141	0.078
E. coli ATCC25922	0.047	0.031	0.031	0.031
E. coli W3110	>0.5[b]	>0.5[b]	0.188	0.078
E. coli mcr-1	0.141	0.078	0.125	0.125
E. coli EQASmcr-1	0.078	0.078	0.094	0.094
E. coli EQASmcr-2	0.094	0.141	0.094	0.125
E. coli EQASmcr-3	0.078	0.078	0.047	0.031

[a]MIC and MSC data can be found in the Supplementary data, Tables S7-12; [b]Synergy is defined in literature as a FICI ≤0.5.[37]

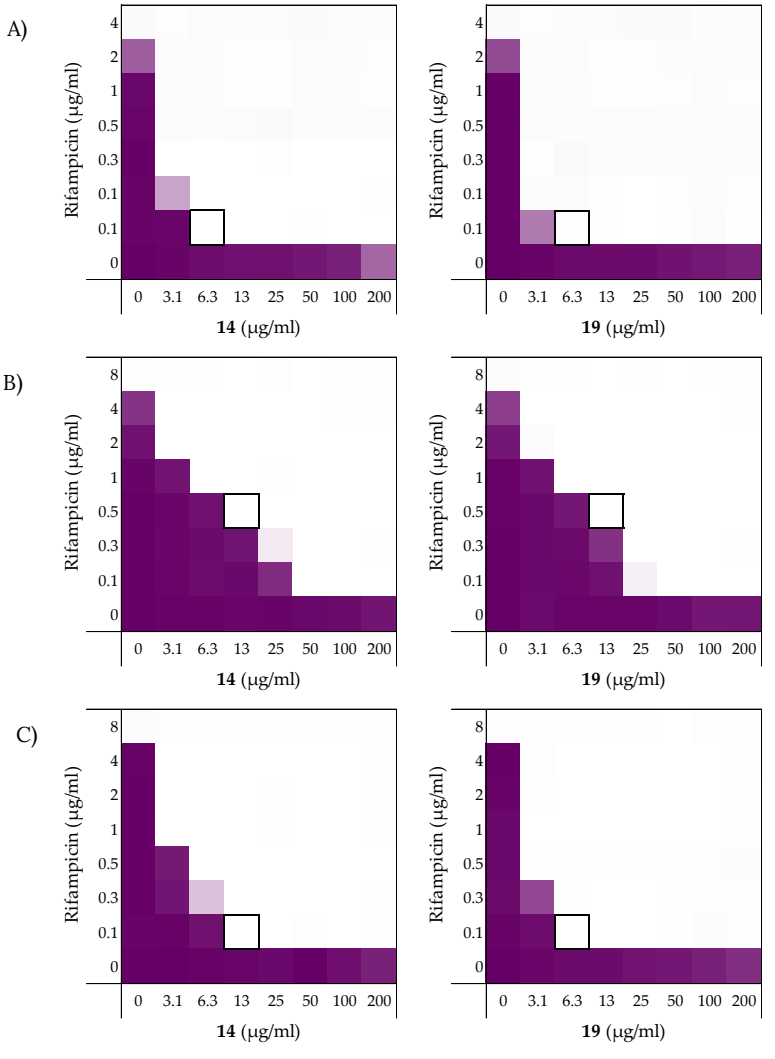

Figure 5. Checkerboard assays of the peptides **14** and **19** in combination with rifampicin versus: A) *E. coli* ATCC25922; and *mcr*-positive isolates B) EQASmcr-1 and C) EQASmcr-3. In each case the bounded box in the checkerboard assays indicates the combination of peptide and antibiotic resulting in the lowest FICI (see Table 4). OD_{600} values were measured using a plate reader and transformed to a gradient: purple represents growth, white represents no growth. Checkerboard assays of peptide **6** and **10** of the strains shown above and all checkerboard assays of *E. coli* W3110, mcr-1 and EQASmcr-2 are available in the Supplementary data, Figure S7-12.

2.3.3. Synergy towards *A. baumannii*, *K. pneumoniae*, and *P. aeruginosa*

After establishing the synergistic potential of peptides **6**, **10**, **14**, and **19** in combination with rifampicin against several *E. coli* strains, we turned our attention to other Gram-negative pathogens. For this part of the study we elected to use laboratory strains *A. baumannii* ATCC17978, *K. pneumoniae* ATCC13883, and *P. aeruginosa* ATCC27853. Rifampicin was again used as the companion antibiotic and we began by establishing its activity against these strains. While a relatively low MIC of 2 μg/mL was measured for rifampicin against the *A. baumannii* ATCC17978 strain, a much lower activity was found against *K. pneumoniae* ATCC13883 and *P. aeruginosa* ATCC27853 where the MICs measured were 32 μg/mL and 16 μg/mL respectively (see Supplementary data, Tables S13–S15).

As illustrated by checkerboard assays of **14** and **19** in Figure 6, all four peptides exhibited potent synergy against the *A. baumannii* and *K. pneumoniae* strains (Table 5). By comparison, significantly less synergy was observed with the *P. aeruginosa* strain with peptide **14** displaying the most potent synergistic activity. The results obtained with *A. baumannii* and *K. pneumoniae* were more in line with our previous findings where again, peptides **14** and **19** resulted in the most potent synergistic combinations with rifampicin. Impressively, a FICI of only 0.023 was detected for both peptides with the *K. pneumoniae* strain tested.

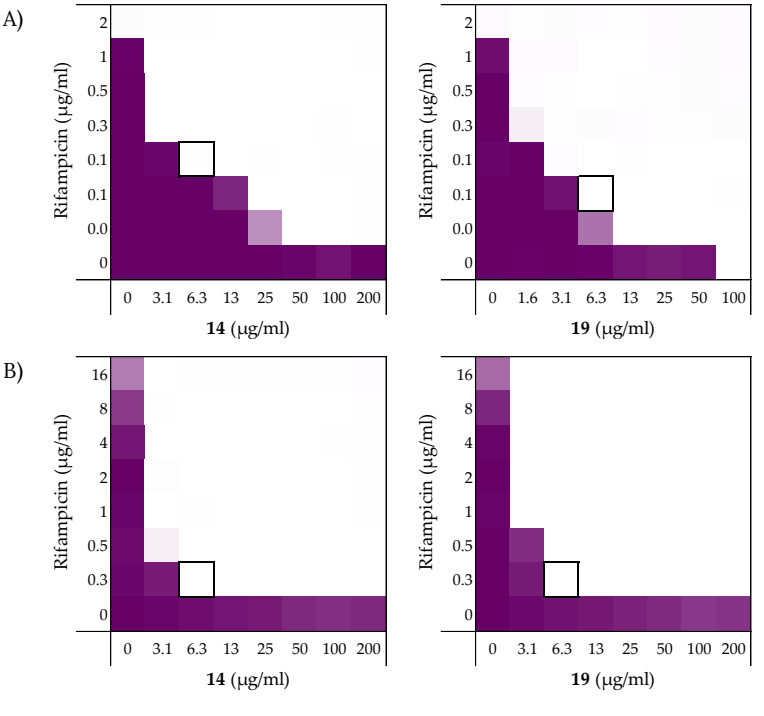

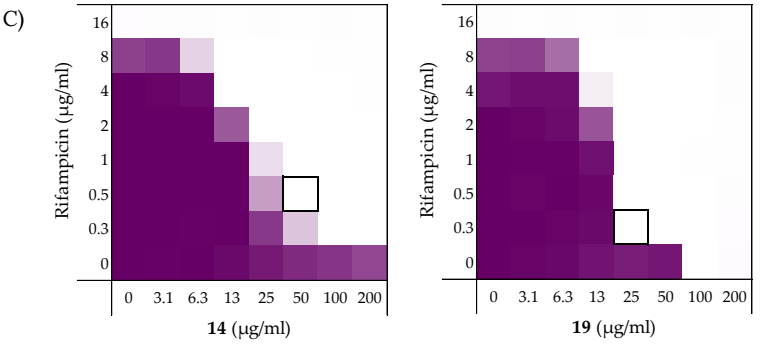

Figure 6. Checkerboard assays for peptides **14** and **19** in combination with rifampicin versus different Gram-negative pathogens: A) *A. baumannii* ATCC17978; B) *K. pneumoniae* ATCC13883; C) *P. aeruginosa* ATCC27853. In each case the bounded box in the checkerboard assays indicates the combination of peptide and antibiotic resulting in the lowest FICI (see Table 5). OD_{600} values were measured using a plate reader and transformed to a gradient: purple represents growth, white represents no growth. Checkerboard assays of peptides **6** and **10** of the strains shown above are available in the Supplementary data, Figures S13-15.

Table 5. FICI values of peptides **6**, **10**, **14**, and **19** in combination with rifampicin against different Gram-negative pathogens.[a]

Pathogen	6	10	14	19
A. baumannii ATCC17978	0.125	0.125	0.078	0.094
K. pneumoniae ATCC13883	0.063	0.063	0.023	0.023
P. aeruginosa ATCC27853	>0.5[b]	0.250	0.156	0.266

[a]MIC and MSC data can be found in the Supplementary data, Tables S13-15; [b]Synergy is defined in literature as a FICI ≤0.5.[37]

2.4. Mechanistic studies

The potentiation of antibiotics like erythromycin, rifampicin, novobiocin and vancomycin against Gram-negative bacteria is generally attained by disruption of the OM as previously described for PMBN.[10] The potent synergy observed for peptides **6**, **10**, **14**, and **19** with these antibiotics, coupled with the finding that the peptides are largely non-hemolytic, points to a mode of action involving selective permeabilization of the Gram-negative OM. To further investigate this hypothesis, a permeabilization assay using N-phenyl-napthalen-1-amine (NPN) on *E. coli* BW25113 was performed. This assay enables monitoring of OM disruption based upon the ability of NPN to enter the phospholipid layer which in turn results in a detectable increase in fluorescence.[47] As illustrated in Figure 7, a clear dose-dependent effect was observed for peptides **6**, **10**, **14**, and **19**. Taken along as a benchmark, PMBN was found to induce ca. 80% OM permeabilization at a concentration of 3.13 μg/mL. By comparison, the peptides matched or surpassed this effect at the higher concentrations tested.

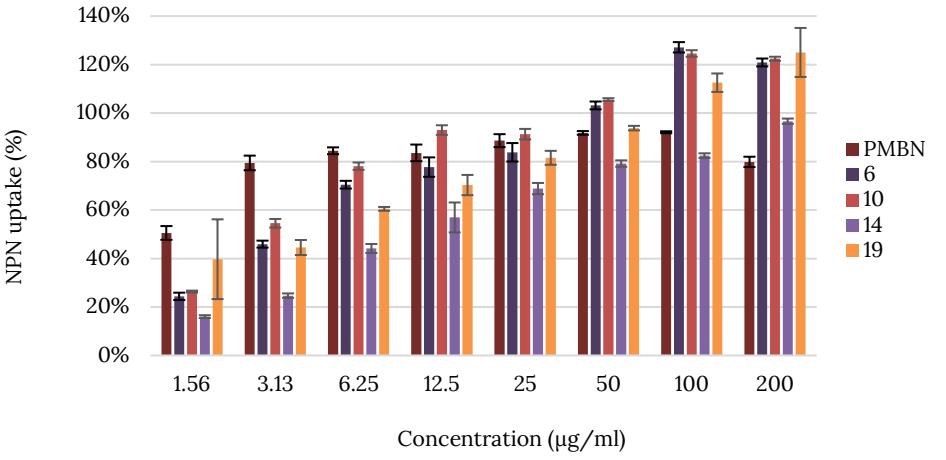

Figure 7. Permeabilization assay of *E. coli* BW25113 using N-Phenyl-1-naphthylamine (NPN) as fluorescent probe. The read-out was performed after 60 minutes of incubation using a plate reader with λ_{ex} 355 nm and λ_{em} 420 nm. The NPN uptake values shown are relative to the uptake signal obtained upon treating the cells with 100 μg/ml colistin as previously reported.[48] Error bars represent the standard deviation based on n=3 technical replicates. A read-out was also performed after 10 minutes of incubation (See Supplementary data, Figure 16).

2.5. Stereochemical studies

We next set out to probe the stereochemical parameters governing the OM disrupting activity of peptides **6**, **10**, **14**, and **19**. The result of the LPS competition assay with peptide **6** (described above in Section 2.1) as well as the published NMR studies on related thrombin-derived C-terminal peptides,[26] suggest that these peptides interact with LPS. At the core of the LPS structure is the bacterial phospholipid lipid A. Given that lipid A is a chiral biomolecule, we next prepared a series of stereochemical analogues of peptide **6** and characterized the impact on synergistic activity. These analogues included the all D-amino acid enantiomeric species **20**, the L-amino acid inverso peptide **21** and the all D-amino acid retro-inverso variant **22**.

Peptide **6** and enantiomer **20** were both found to exhibit appreciable inherent antimicrobial activity against *E. coli* BW25113, with MICs of 12.5 μg/mL and 6.25 μg/mL respectively (Table 6). Inversion of these peptides to give **21** and **22** led to a significant loss of antibacterial activity in both cases with MICs of >200 μg/mL and 100 μg/mL respectively. Checkerboard assays were next performed with erythromycin as the companion antibiotic using *E. coli* BW25113 as the indicator strain (Figure 8). Interestingly, the enantiomeric peptide **20** was found to exhibit no synergistic activity suggesting that the synergy observed for **6** is indeed stereospecific. Interestingly, the L-inverso peptide **21** did exhibit moderate synergistic activity, however, the D-retro-inverso peptide **22** was a much more potent synergist. Give that retro-inverso peptides can assume a side chain topology similar to that of the parent L-peptide,[49] these finding further support the stereospecific mechanism of peptide **6**. Similar results were obtained upon repeating the synergy assays for peptides **6**, **20–22** with rifampicin as the companion antibiotic (see Supplementary data, Figure S2 and Table S2).

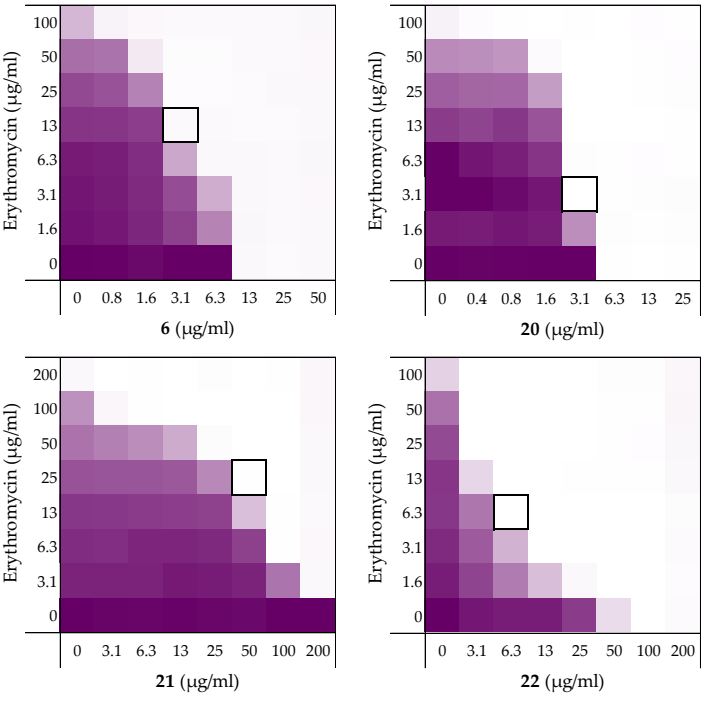

Figure 8. Checkerboard assays of the peptides **6**, and stereochemical analogues **20**-**22** in combination with erythromycin versus *E. coli* BW25113. In each case the bounded box in the checkerboard assays indicates the combination of peptide and antibiotic resulting in the lowest FICI (see Table 1). OD_{600} values were measured using a plate reader and transformed to a gradient: purple represents growth, white represents no growth. An overview of all checkerboard assays with erythromycin can be found in the Supplementary data, Figure S1.

Table 6. Overview of the TCPs peptide sequence, synergistic and hemolytic activity.

	Peptide sequence[a]	MIC	$MSC_{peptide}$	FICI	Hemolysis[c]
6	H_2N-VFRLKKWIQKVI-NH_2	12.5	3.13	0.313	4%
20	H_2N-vfrlkkwiqkvi-NH_2	6.25	3.13	>0.5[b]	3%
21	H_2N-IVKQIWKKLRFV-NH_2	>200	50	0.250	2%
22	H_2N-ivkqiwkklrfv-NH_2	100	6.25	0.094	3%

[a]Lower case letters indicate D-amino acids; [b]Synergy defined as an FICI ≤0.5[37]; [c]Hemolysis determined after a 20 hour incubation of the compounds (200 μg/ml) with defibrinated sheep blood (see Supplementary data, Figure S4 and Table S4).

3. Discussion

The LPS-binding potential of the TCPs sparked our interest in these peptides as potential synergists. Indeed, the synergistic activity of peptides **1**, **2**, and **3** validated this hypothesis (See Table 2). Notably, this represents the first demonstration of the synergistic activity for these peptides even though their antimicrobial activity has been well-studied.[26,35,36,50–52] Peptide **1** exhibits synergy comparable to PMBN (Table 1). Amidation of the C-terminus of peptide **1** gave peptide **6** and led to a significant enhancement of inherent antibiotic activity, an effect also known for other antimicrobial peptides.[53] Most importantly, peptide **6** maintained synergistic activity leading to the lowest MSC and was therefore selected as a lead for further investigation.

While C-terminal amidation impacts the overall charge in peptide **6**, LPS-binding is still maintained as evidenced by the results of an LPS competition assay (Supplementary data, Figure S4 and Table S4). Moreover, stereochemical studies with peptide **6** suggests that synergistic activity is indeed stereospecific: loss of synergistic activity was observed for the mirror image of peptide **6**, D-peptide **20** (see Table 6). Similarly, in literature the mirror image of PMBN was described to have no synergistic activity.[54] Notable, however, is the finding that retro-inverso peptide **22** displays potent synergistic activity, in line with expectations given that the retro-inverso analogue features a topology similar to parent peptide **6**.[49]

Another indication of a mechanism involving LPS-binding comes from the antimicrobial activity observed for peptide **6** against wild-type and *mcr*-1 strains of *E. coli*: while MIC values of 12.5 μg/mL and 6.25 μg/mL where measured against the reference BW25113 and W3110 strains, respectively, in the case of the *mcr*-1,2,3 clinical isolates tested the MICs were much higher (50–100 μg/mL, see Supplementary data, Tables S2, S8–S12). A similar trend is also observed for the established LPS-binding polymyxin class of antibiotics.[45,46] Interestingly, the synergistic activity of peptide **6**, and the alanine-scan derived analogues **10**, **14**, and **19** is well retained against *mcr*-type stains which is not the case for PMBN (Table 4).[31]

The alanine scan provided insight into the roles of each amino acid in peptide **6** and resulted in the identification of three potent synergists: peptide **10**, **14**, and **19** (Table 2). All three peptides potentiated erythromycin, rifampicin, novobiocin, and vancomycin (Table 2 and Table 3). Peptide **19** was on par with PMBN and results in lower or equal FICIs of synergists recently described in literature.[31,33] Impressively, the potentiation of rifampicin by peptide **14** and **19** was also seen against multiple *E. coli* strains including the *mcr*-clinical isolates, *K. pneumoniae*, *P. aeruginosa*, and *A. baumannii* also with very low FICI values (Table 4 and Table 5). By comparison, peptide **10** displayed a slightly lower synergistic activity than peptide **14** and **19**, but was still equal to or better than peptide **6**. Interestingly, peptide **14** features the substitution of Ala for Trp, a residue often associated with membrane binding and antimicrobial activity.[55–58] Indeed, a significant loss of inherent antimicrobial activity is observed for peptide **14** relative to **6**. However, the finding that peptide **14** retains potent synergy suggests the Trp is not key for synergistic activity or OM permeabilization (Figure 7).

What is also clear from the alanine scan is the essentiality of the lysine side-chains, not only for maintaining synergy, but also for limiting hemolytic activity (Table 2). Comparable findings have been reported for PMB and PMBN which contain several positively charged Dab resides and replacing them with uncharged amino acids leads to a loss of antimicrobial activity for PMB and synergistic activity for PMBN.[59]

In summary, the peptides investigated in this study were found to exhibit potent and targeted synergy with multiple Food and Drug Administration (FDA)-approved Gram-positive-specific antibiotics. Importantly, this synergy was demonstrated against a range of Gram-negative species including *mcr*-resistant strains. The selective OM disrupting properties of these peptides and their potent synergy highlights the potential for such compounds to expand the number of antibiotic classes that can be effectively employed to kill Gram-negative bacteria.

4. Experimental section

4.1. Manual Peptide Synthesis for Carboxylic Acid C-terminus

Chlorotrityl resin (5.0 g, 1.60 mmol·g−1) was loaded with Fmoc-Ile-OH (1, 5) or Fmoc-Glu(OtBu)-OH (2-4). Resin loading was determined to be 0.44–0.57 mmol·g−1. Linear peptide encompassing the first amino acid until the last amino acid were assembled manually via standard Fmoc solid-phase peptide synthesis (SPPS) (resin bound AA:Fmoc-AA:BOP:DiPEA, 1:4:4:8 molar eq.) on a 0.1 mmol scale. DMF was used as solvent and Fmoc deprotections were carried out with piperidine:DMF (1:4 v:v). Amino acid side chains were protected as follows: tBu for Asp/Glu, Trt for Asn/Gln, Boc for Lys/Trp, Pbf for Arg. Following coupling and Fmoc deprotection of the final amino acid, N-terminal acylation was achieved for peptide 5 by coupling Ac2O using the same coupling conditions used for SPPS. The resin-bound peptides were next washed with CH2Cl2 and subsequently treated with TFA:TIS:H2O (95:2.5:2.5, 10 mL) for 90 min. Resin beads were filtered off and the reaction mixture was added to cold MTBE:hexanes (1:1) and the resulting precipitate washed once more with MTBE:hexanes (1:1). The crude peptide was lyophilized from tBuOH:H2O (1:1) and purified with reverse phase HPLC. Pure fractions were pooled and lyophilized to yield the desired linear peptides as white powders, typically in 10–20 mg quantities. For peptide characterization and analysis see Supplementary data, Table S16 and pages S26–S28.

4.2. Automated Peptide Synthesis for C-terminal Amides

Rink Amide resin (150 mg, 0.684 mmol·g−1) was loaded into the reaction vessel of the CEM liberty blue peptide synthesizer for a 0.1 mmol scale. Linear peptides 6–22 were assembled using microwave irradiation at 90 C (resin bound AA:Fmoc-AA:DIC:Oxyma, 1:5:5:5 molar eq.). DMF was used as solvent and Fmoc deprotections were carried out with piperidine:DMF (1:4, v:v). Amino acid side chains were protected as follows: tBu for Asp/Glu, Trt for Asn/Gln, Boc for Lys/Trp, Pbf, for Arg. Following coupling and Fmoc deprotection of the final amino acid, N-terminal acylation was achieved for peptide 7 by coupling Ac2O using microwave irradiation at 90 C. The linear peptides were removed from the reaction vessel, washed with DCM and directly treated with TFA:TIS:H2O (95:2.5:2.5, 10 mL) for 90 min. Resin beads were filtered off and the reaction mixture was added to cold MTBE:hexanes (1:1) and the resulting precipitate washed once more with MTBE:hexanes (1:1). The crude peptides was lyophilized from tBuOH:H2O (1:1) and purified with reverse phase HPLC. Pure fractions were pooled and lyophilized to yield the desired linear peptides as white powders, typically in 20–60 mg quantities. For peptide characterization and analysis see Supplementary data.

4.3. Antimicrobial Assays

All peptides were screened for antimicrobial activity against *E. coli* BW25113, *E. coli* ATCC25922, and *E. coli* W3110. A select group of the peptides was further tested against *E. coli* mcr-1, *E. coli* EQASmcr-1, *E. coli* EQASmcr-2, *E. coli* EQASmcr-3, *K. pneumoniae* ATCC13883, *P. aeruginosa* ATCC27853, and *A. baumannii* ATCC17978. The antimicrobial assay was performed according to CLSI guidelines. Bacteria were plated out directly from their glycerol stocks on blood agar plates, incubated overnight at 37 °C, and then kept in the fridge. The blood agar plates were only used for 2 weeks and then replaced.

4.4. Minimum Inhibitory Concentration (MIC) Assay

A single colony from a blood agar plate was inoculated in Lysogeny Broth (LB) at 37 °C until a 0.5 optical density at 600nm (OD600) was reached (compared to the sterility control of LB). The bacterial suspension was diluted in fresh LB to 2.0 x 10^6 CFU/mL. The serial dilutions were prepared in polypropylene microtiter plates: a stock of the test compounds was prepared with a 2x final concentration in LB. 100 µl of the stock was added to the wells of the top row of which 50 µl was

used for the serial dilution. The bottom row of each plate was used as the positive (50 µl of LB) and negative controls (100 µl of LB) (6 wells each). 50 µl of the 2.0 x 106 CFU/mL bacterial stock was added to each well except for the negative controls, adding up to a total volume of 100 µl per well. The plates were sealed with a breathable seal and incubated for 20 hours at 37 °C and 600 rpm. The MIC was visually determined after centrifuging the plates for 2 minutes at 3000 rpm.

4.5. Checkerboard Assays

Dilution series of both the test compound and antibiotic to be evaluated was prepared in LB media. To evaluate synergy, 25 µL of the test compound solutions were added to wells containing 25 µL of the antibiotic solution. This was replicated in three columns for each combination so as to obtain triplicates. To the resulting 50 µL volume of antibiotic + test compound was next added 50 µL of bacterial stock and the plates sealed. After incubation for 20 hours at 37 °C while shaking at 600 rpm, the breathable seals were removed and the plates shaken using a bench top shaker to ensure even suspension of the bacterial cells as established by visual inspection. The plates were then transferred to a Tecan Spark plate reader and following another brief shaking (20 seconds) the density of the bacterial suspensions measured at 600 nm (OD600). The resulting OD600 values were transformed to a 2D gradient to visualize the growth/no-growth results. The FICI was calculated using Equation 1 where a FICI ≤0.5 indicating synergy.[37]

$$\mathrm{FICI} = \frac{\mathrm{MSC_{ant}}}{\mathrm{MIC_{ant}}} + \frac{\mathrm{MSC_{syn}}}{\mathrm{MIC_{syn}}} \quad (1)$$

Equation 1. Calculation of the FICI: Calculation of FICI. MSC_{ant} = MIC of antibiotic in combination with synergist; MIC_{ant} = MIC of antibiotic alone; MSC_{syn} = MIC of synergist in combination with antibiotic; MIC_{syn} = MIC of synergist alone. In cases where the MIC of the antibiotic or synergist was found to exceed the highest concentration tested, the next highest concentration in the dilution series was used in determing the FICI and the result reported as ≤ the calculated value.

4.6. Hemolysis Assay

The hemolytic activity of each analogue was assessed in triplicate. Red blood cells from defibrillated sheep blood obtained from Thermo Fisher were centrifuged (400 g for 15 minutes at 4°C) and washed with Phosphate-Buffered Saline (PBS) containing 0.002% Tween20 (buffer) for five times. Then, the red blood cells were normalized to obtain a positive control read-out between 2.5 and 3.0 at 415 nm to stay within the linear range with the maximum sensitivity. A serial dilution of the compounds (200 – 6.25 µg/mL, 75 µL) was prepared in a 96-well plate. The outer border of the plate was filled with 75 µL buffer. Each plate contained a positive control (0.1% Triton-X final concentration, 75 µL) and a negative control (buffer, 75 µL) in triplicate. The normalized blood cells (75 µL) were added and the plates were incubated at 37 °C for 1 hour or 20 hours while shaking at 500 rpm. A flat-bottom plate of polystyrene with 100 µL buffer in each well was prepared. After incubation, the plates were centrifuged (800 g for 5 minutes at room temperature) and 25 µL of the supernatant was transferred to their respective wells in the flat-bottom plate. The values obtained from a read-out at 415 nm were corrected for background (negative control) and transformed to a percentage relative to the positive control.

4.7. LPS Competition Assay

The same protocol as the MIC assay was used to prepare the serial dilution of the compounds in 96-wells plates in duplicate resulting in two identical plates. A serial dilution of colistin was taken along as a control. The inoculation and preparation of the bacteria stock was performed as described for the MIC assay. The stock of bacteria was then split into two stocks. LPS (1 mg/mL final

concentration) was added to one of the stocks and added to one of the duplicate plates as described in the MIC assay. The normal bacteria stock was added to the remaining plate as described in the MIC assay. The plates were sealed with a breathable seal and incubated for 20 h at 37 °C and 600 rpm after which the MIC was visually determined.

4.8. Membrane Permeability Assay Using N-phenylnaphthalen-1-amine (NPN)

The assay was performed based on protocols adapted from those described in literature.[47,48] Bacteria were inoculated overnight at 37 °C in LB, diluted the next day 50x in LB and grown to OD600 of 0.5. The bacterial suspension was then centrifuged for 10 minutes at 1000 g at 25 °C. The pellet of bacteria was suspended in 5 mM HEPES buffer containing 20 mM glucose to a final concentration of OD600 of 1.0. The compounds were serial diluted (25 µL) in triplicate in a black ½ area clear-bottom 96-well plate. 100 µg/mL final concentration of colistin in triplicate served as the positive control. Three wells were filled with 25 µL buffer to serve as the negative control. Additional controls of the compounds were made in triplicate using 25 µl of the highest concentration to detect interactions of the compounds with NPN in the absence of bacteria. A stock of 0.5 mM of NPN in acetone was prepared and diluted 12.5x in the buffer. 25 µL of the NPN solution was added to each well. 50 µL of the 1.0 OD_{600} bacterial stock was then added to each well except for the controls of the compounds with NPN. To these wells 50 µL of buffer was added. After 60 minutes the plate was measured using Tecan plate reader with λ_{ex} 355 nm ±20 nm and λ_{em} 420 nm ±20 nm. The fluorescence values obtained were then transformed into a NPN uptake percentage using the following equation 2:

$$\text{NPN uptake (\%)} = (F_{obs} - F_0) / (F_{100} - F_0) \times 100\%, \quad (2)$$

Equation 2. consists of an observed value of fluorescence (Fobs), which is corrected for background using the negative control (F0). This value is divided by the positive control corrected for background (F100–F0) and multiplied by 100% to obtain the percentage.[48,60]

Supplementary data

General notes

All reagents employed were of American Chemical Society (ACS) grade or finer and were used without further purification unless otherwise stated. For compound characterization HRMS analysis was performed on a Shimadzu Nexera X2 UHPLC system with a Waters Acquity HSS C18 column (2.1 × 100 mm, 1.8 µm) at 30 °C and equipped with a diode array detector. The following solvent system, at a flow rate of 0.5 mL/min, was used: solvent A, 0.1 % formic acid in water; solvent B, 0.1 % formic acid in acetonitrile. Gradient elution was as follows: 95:5 (A/B) for 1 min, 95:5 to 15:85 (A/B) over 6 min, 15:85 to 0:100 (A/B) over 1 min, 0:100 (A/B) for 3 min, then reversion back to 95:5 (A/B) for 3 min. This system was connected to a Shimadzu 9030 QTOF mass spectrometer (ESI ionisation) calibrated internally with Agilent's API-TOF reference mass solution kit (5.0 mM purine, 100.0 mM ammonium trifluoroacetate and 2.5 mM hexakis(1H,1H,3H-tetrafluoropropoxy)phosphazine) diluted to achieve a mass count of 10000. Purity of the peptides was confirmed to be ≥ 95% by analytical RP-HPLC using a Shimadzu Prominence-i LC-2030 system with a Dr. Maisch ReproSil Gold 120 C18 column (4.6 × 250 mm, 5 µm) at 30 °C and equipped with a UV detector monitoring at 214 nm. The following solvent system, at a flow rate of 1 mL/min, was used: solvent A, 0.1 % TFA in water/acetonitrile, 95/5; solvent B, 0.1 % TFA in water/acetonitrile, 5/95. Gradient elution was as follows: 95:5 (A/B) for 2 min, 95:5 to 0:100 (A/B) over 13 min, 0:100 (A/B) for 2 min, then reversion back to 95:5 (A/B) over 1 min, 95:5 (A/B) for 2 min. The compounds were purified via preparative HPLC using a BESTA-Technik system with a Dr. Maisch Reprosil Gold 120 C18 column (25 × 250 mm, 10 µm) and equipped with a ECOM Flash UV detector monitoring at 214 nm. The following solvent system, at a flow rate of 12 mL/min, was used: solvent A, 0.1 % TFA in water/acetonitrile 95/5; solvent B, 0.1 % TFA in water/acetonitrile 5/95. Gradient elution was as follows: 95:5 (A/B) for 2 min, 95:5 to 0:100 (A/B) over 30 min, 0:100 (A/B) for 2 min, then reversion back to 95:5 (A/B) over 1 min, 95:5 (A/B) for 2 min.

Peptide synthesis

Automated peptide synthesis. Peptides were synthesized by a microwave-assisted peptide synthesizer (Liberty Blue HT-12, CEM) using the following cycles of deprotection and coupling.

1) Fmoc deprotection: 90 °C, 80 W, 65 s with 20% piperidine in DMF, 3 mL/deprotection

2) AA coupling: Fmoc-AA-OH (0.2M in 2.5 mL DMF, 5 eq), DIC (1M in 1 mL DM, 10 eq) and Oxyma (1M in 0.5 mL DMF, 5 eq) at 76 °C, 80 W, 15 s before the temperature was increased to 90 °C, 80 W for 110s.

Synthesis of C-terminal acid peptides.

Chlorotrityl resin was loaded with the first Fmoc-AA-OH (depending on the sequence). Linear peptide encompassing the first AA to the last AA was assembled manually via standard Fmoc solid-phase peptide synthesis (SPPS) (resin bound AA:Fmoc-AA:BOP:DiPEA, 1:4:4:8 molar eq.) on a 0.25 mmol scale. DMF was used as solvent and Fmoc deprotections were carried out with piperidine:DMF (1:4 v:v). Amino acid side chains were protected as follows: tBu for Ser/Asp/Glu/Tyr, Trt for Asn/Gln/His, Boc for Lys/Trp, and Pbf for Arg. Following coupling and Fmoc deprotection of the final AA, the resin was directly treated with TFA:TIS:H2O (95:2.5:2.5, 10 mL) for 90 min. The reaction mixture was added to cold MTBE:hexanes (1:1) and the resulting precipitate was centrifuged at 4500 rpm for 5 min, washed once more with MTBE:hexanes (1:1) and centrifuged at 4500 rpm for 5 min. The crude peptides were lyophilized from tBuOH:H2O (1:1) and purified with reverse phase HPLC. Pure fractions were pooled and lyophilized to yield the desired linear peptide products in >95% purity as white powders.

Synthesis of C-terminal amide peptides.
Rink Amide resin (150 mg, 0.684 mmol.g-1) was loaded into the CEM Liberty Blue peptide synthesizer for a 0.1mmol scale. Linear peptide encompassing the first amino acid to the last amino acid were assembled using microwave irradiation (resin bound AA:Fmoc-AA:DIC:Oxyma, 1:5:10:5 molar eq.). DMF was used as solvent and Fmoc deprotections were carried out with piperidine:DMF (1:4, v:v). Amino acid side chains were protected as follows: tBu for Ser/Asp/Glu/Tyr, Trt for Asn/Gln/His, Boc for Lys/Trp, and Pbf for Arg. Following coupling and Fmoc deprotection of the final AA, the resin was directly treated with TFA:TIS:H2O (95:2.5:2.5, 10 mL) for 90 min. The reaction mixture was added to cold MTBE:hexanes (1:1) and the resulting precipitate was centrifuged at 4500 rpm for 5 min, washed once more with MTBE:hexanes (1:1) and centrifuged at 4500 rpm for 5 min. The crude peptides were lyophilized from tBuOH:H2O (1:1) and purified with reverse phase HPLC. Pure fractions were pooled and lyophilized to yield the desired linear peptide products in >95% purity as white powders.

Checkerboard assays and FICI data against *E. coli* BW25113 with rifampicin

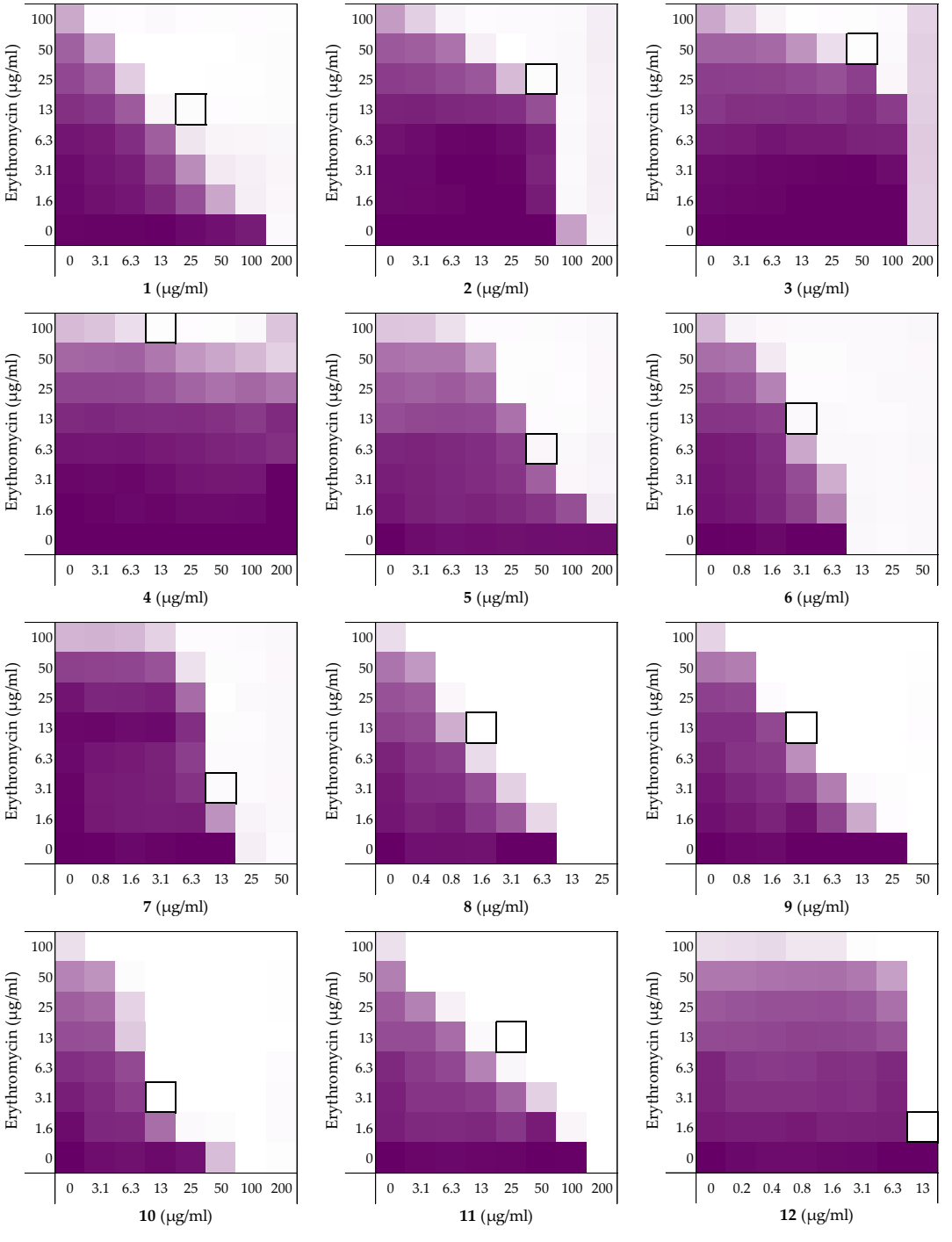

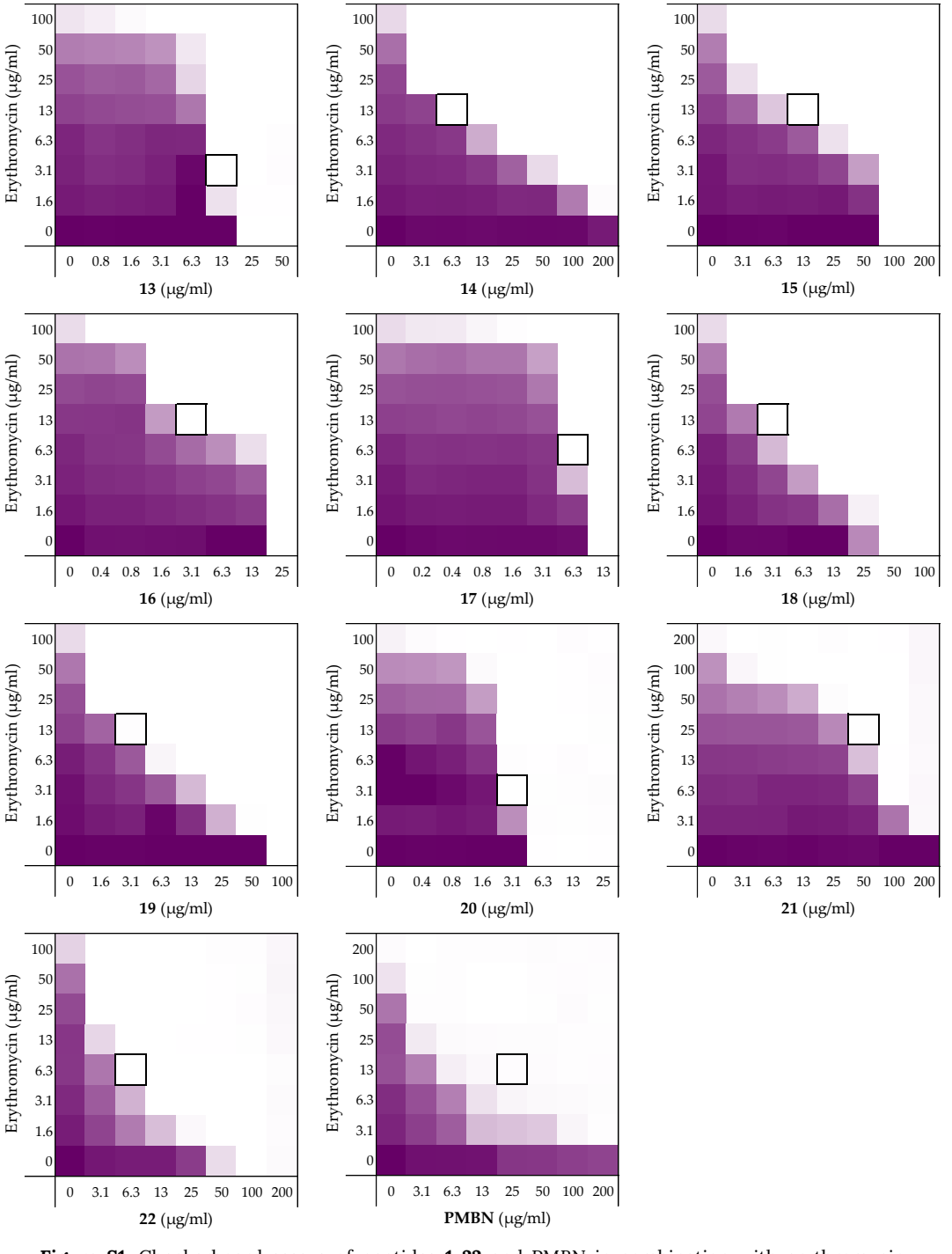

Figure S1. Checkerboard assays of peptides **1**-**22** and PMBN in combination with erythromycin versus *E. coli* BW25113. OD600 values were measured using a plate reader and transformed to a gradient: purple represents growth, white represents no growth. In each case, the bounded box in

the checkerboard assays indicates the minimal synergistic concentration (MSC) of compound and antibiotic resulting in the lowest FICI.

Table S1. Synergistic data of peptides **1-22** and PMBN of the checkerboard assays with erythromycin as shown in Figure S1. All minimal inhibitory concentrations (MICs) and minimal synergistic concentrations (MSCs) are in μg/mL.

	MIC_{pep}	MSC_{pep}	MIC_{ery}	MSC_{ery}	FICI
1	200	25	>100	12.5	0.1875
2	200	50	>100	25	0.3750
3	200	50	>100	50	0.5000
4	>200	12.5	>100	100	>0.5[a]
5	>200	50	>100	6.25	0.1563
6	12.5	3.125	>100	12.5	0.3125
7	50	12.5	>100	3.125	0.2656
8	12.5	1.563	>100	12.5	0.1875
9	50	3.125	>100	12.5	0.1250
10	100	12.5	>100	3.125	0.1406
11	200	25	>100	12.5	0.1875
12	25	12.5	>100	1.563	>0.5[a]
13	25	12.5	>100	3.125	>0.5[a]
14	>200	6.25	>100	12.5	0.0781
15	100	12.5	>100	12.5	0.1875
16	25	3.125	>100	12.5	0.1875
17	12.5	6.25	>100	6.25	>0.5[a]
18	50	3.125	>100	12.5	0.1250
19	100	3.125	>100	12.5	0.0938
20	6.25	3.13	>100	3.125	>0.5[a]
21	>200	50	200	25	0.2500
22	100	6.25	>100	6.25	0.0938
PMBN	>200	25	200	12.5	0.1250

[a] Synergy is defined as FICI ≤0.5.[37]

Checkerboard assays and FICI data against *E. coli* BW25113 with rifampicin

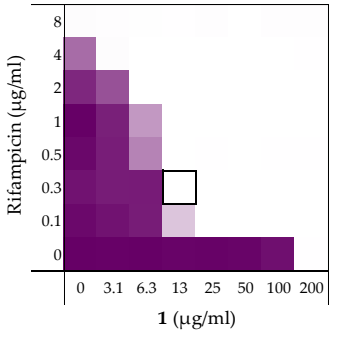

1 (μg/ml)

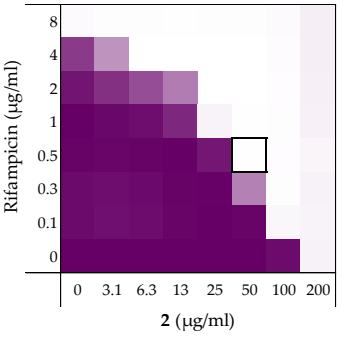

2 (μg/ml)

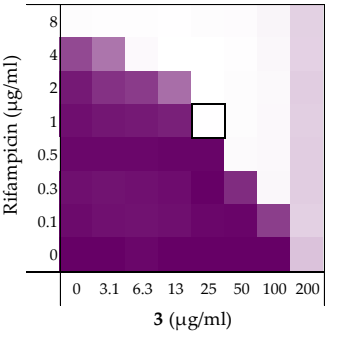

3 (μg/ml)

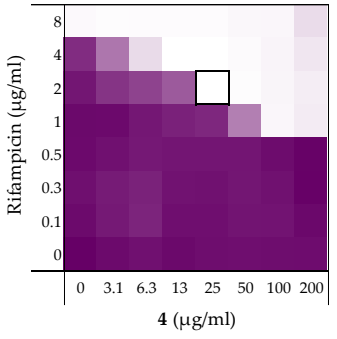

4 (μg/ml)

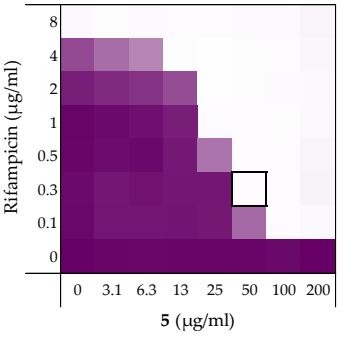

5 (μg/ml)

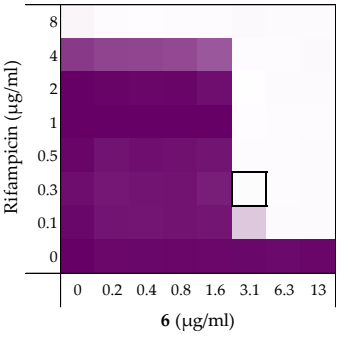

6 (μg/ml)

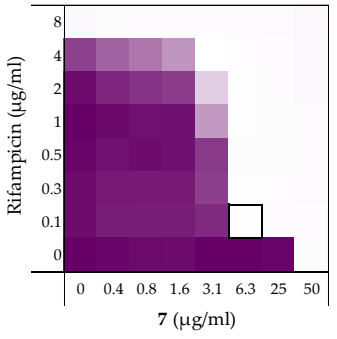

7 (μg/ml)

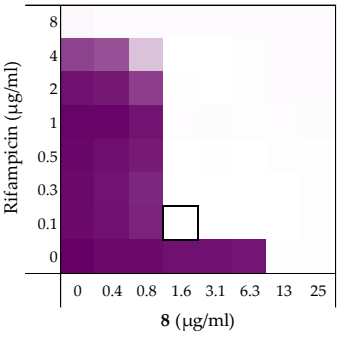

8 (μg/ml)

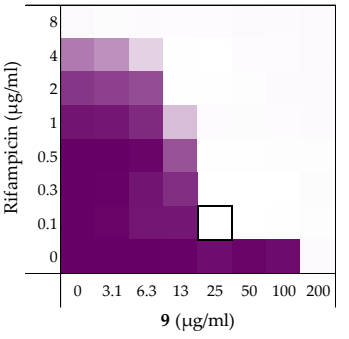

9 (μg/ml)

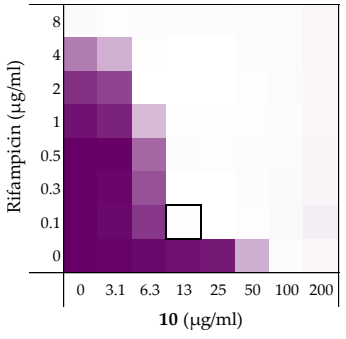

10 (μg/ml)

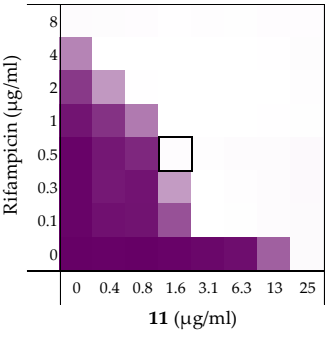

11 (μg/ml)

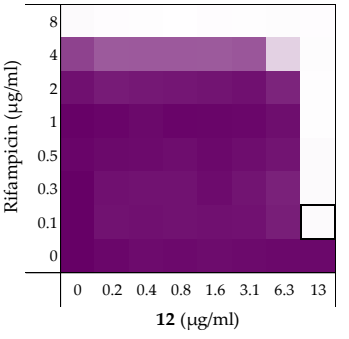

12 (μg/ml)

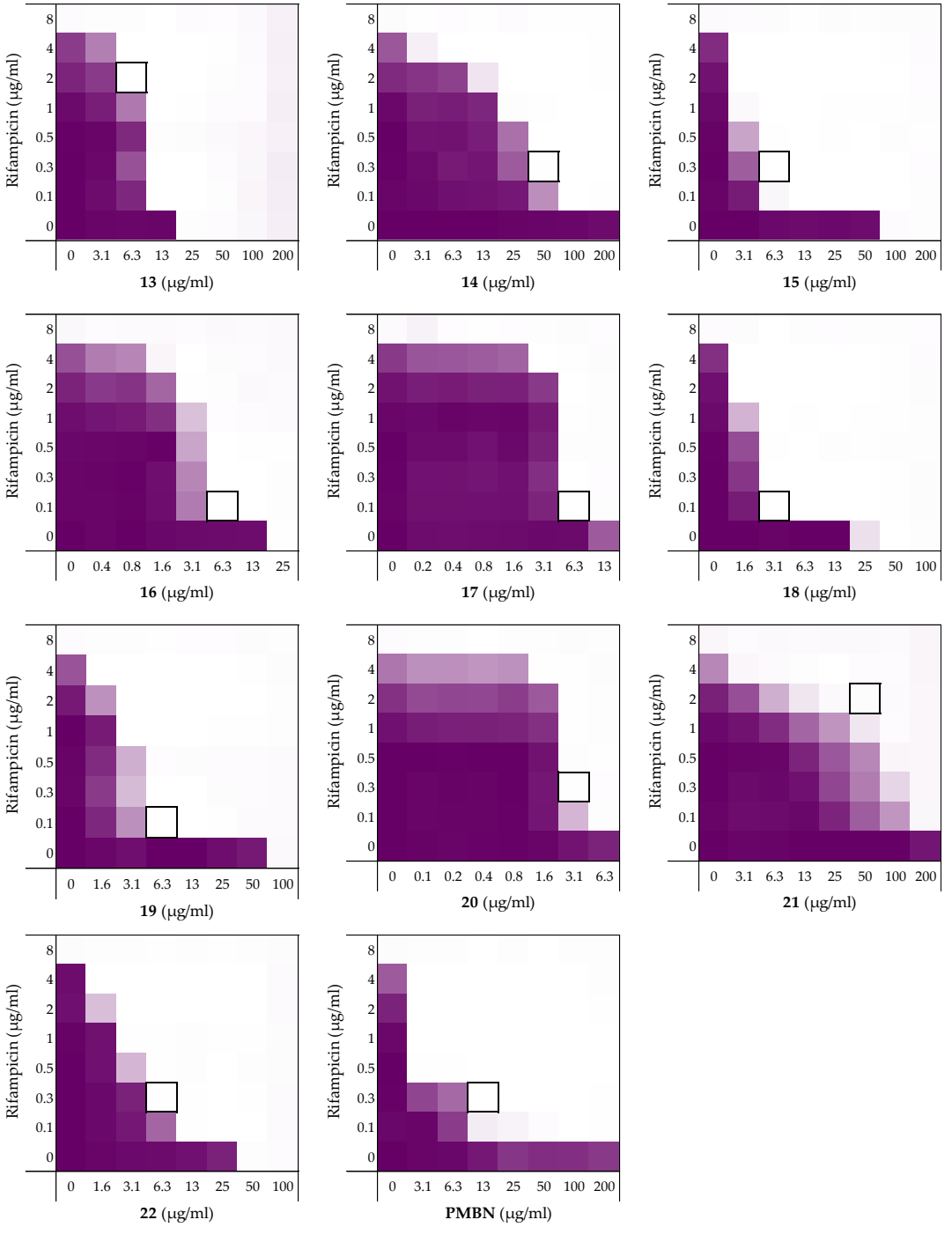

Figure S2. Checkerboard assays of peptides **1**-**22** and PMBN in combination with rifampicin versus *E. coli* BW25113. OD600 values were measured using a plate reader and transformed to a gradient: purple represents growth, white represents no growth. In each case, the bounded box in the

checkerboard assays indicates the minimal synergistic concentration (MSC) of compound and antibiotic resulting in the lowest FICI.

Table S2. Synergistic data of peptides **1**–**22** and PMBN of the checkerboard assays with erythromycin as shown in Figure S2. All minimal inhibitory concentrations (MICs) and minimal synergistic concentrations (MSCs) are in μg/mL.

	MIC_{pep}	MSC_{pep}	MIC_{rif}	MSC_{rif}	FICI
1	200	12.5	8	0.25	0.0938
2	200	50	8	0.5	0.3125
3	>200	25	8	1	0.1875
4	>200	25	8	2	0.3125
5	>200	50	8	0.25	0.1563
6	25	3.125	8	0.25	0.1563
7	50	12.5	8	0.125	0.2656
8	12.5	1.563	8	0.125	0.1406
9	200	25	8	0.125	0.1406
10	100	12.5	8	0.125	0.1406
11	25	1.563	8	0.5	0.1250
12	25	12.5	8	0.125	>0.5[a]
13	25	6.25	8	2	0.5000
14	>200	50	8	0.125	0.1406
15	100	6.25	8	0.25	0.0938
16	25	6.25	8	0.125	0.2656
17	25	6.25	8	0.125	0.2656
18	50	3.125	8	0.125	0.0781
19	100	6.25	8	0.125	0.0781
20	12.5	3.125	8	0.25	0.2813
21	>200	50	8	2	0.3750
22	50	6.25	8	0.25	0.1406
PMBN	>200	12.5	8	0.25	0.0625

[a] Synergy is defined as FICI ≤0.5.[37]

LPS competition assay of peptide 6

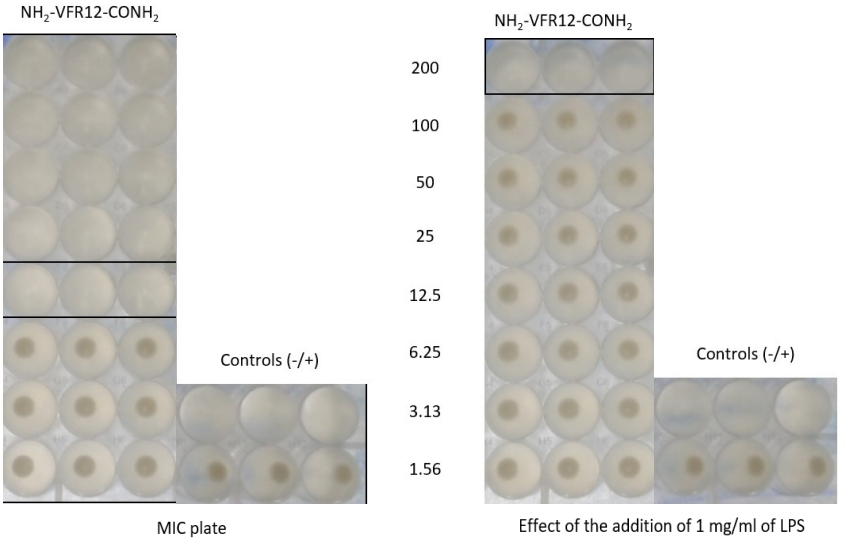

Figure S3. LPS competition assay of **6** with *E. coli* BW25113 in LB as described in materials and methods. A visual read-out was performed after centrifuging the plates for 2 minutes at 3000 rpm.

Table S3. Overview of LPS competition results using LB as medium. All results are obtained against *E. coli* BW25113 as shown in Figure S4.

	Peptide sequence	MIC	+ 1.0 mg/ml LPS
6	H_2N-VFRLKKWIQKVI-NH_2	12.5	200

Hemolysis assay

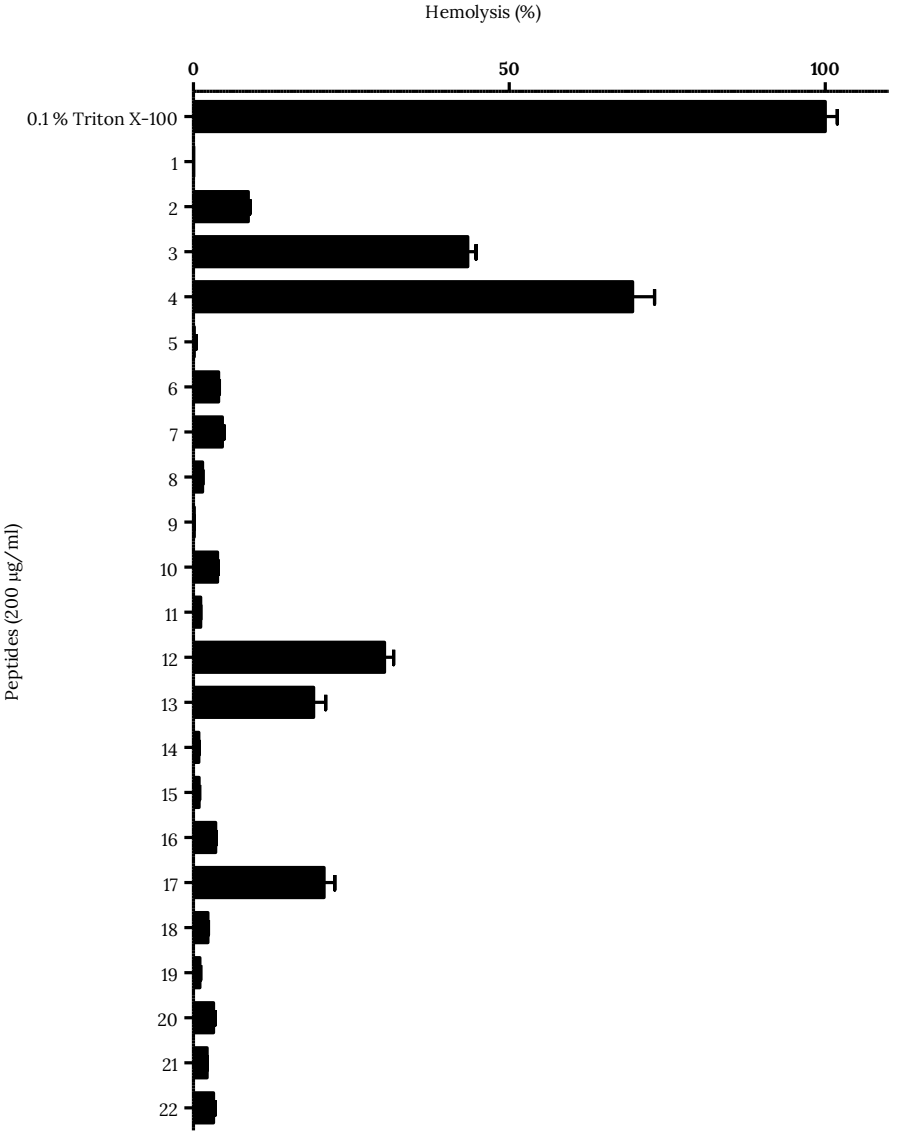

Figure S4. Hemolytic activity of peptides **1-22** (200 µg/ml). The hemolysis assay was performed as described in materials and methods. Values above 10% were defined as hemolytic for the peptides **1-4** in a previous study.[35] Error bars represent the standard deviation based on n=3 technical replicates.

Table S4. Hemolytic activity of peptides **1–22** (200 µg/ml). The hemolysis assay was performed as described in materials and methods. Values >10% were defined as hemolytic for the peptides **1–4** in a previous study.[35]

Compound	**Peptide sequence**	**Hemolysis (%)**
1	H_2N-VFRLKKWIQKVI-OH	0.1
2	H_2N-HVFRLKKWIQKVIDQFGE-OH	8.7
3	H_2N-FYTHVFRLKKWIQKVIDQFGE-OH	43.4
4	H_2N-GKYGFYTHVFRLKKWIQKVIDQFGE-OH	69.5
5	Ac-VFRLKKWIQKVI-OH	0.2
6	H_2N-VFRLKKWIQKVI-NH_2	4.0
7	Ac-VFRLKKWIQKVI-NH_2	4.6
8	H_2N-**A**FRLKKWIQKVI-NH_2	1.5
9	H_2N-V**A**RLKKWIQKVI-NH_2	0.1
10	H_2N-VF**A**LKKWIQKVI-NH_2	3.8
11	H_2N-VFR**A**KKWIQKVI-NH_2	1.1
12	H_2N-VFRL**A**KWIQKVI-NH_2	30.2
13	H_2N-VFRLK**A**WIQKVI-NH_2	19.0
14	H_2N-VFRLKK**A**IQKVI-NH_2	0.9
15	H_2N-VFRLKKW**A**QKVI-NH_2	0.9
16	H_2N-VFRLKKWI**A**KVI-NH_2	3.5
17	H_2N-VFRLKKWIQ**A**VI-NH_2	20.7
18	H_2N-VFRLKKWIQK**A**I-NH_2	2.3
19	H_2N-VFRLKKWIQKV**A**-NH_2	1.0
20	H_2N-vfrlkkwiqkvi-NH_2	3.2
21	H_2N-IVKQIWKKLRFV-NH_2	2.2
22	H_2N-ivkqiwkklrfv-NH_2	3.2

Checkerboard assays and FICI data against *E. coli* BW25113 with novobiocin

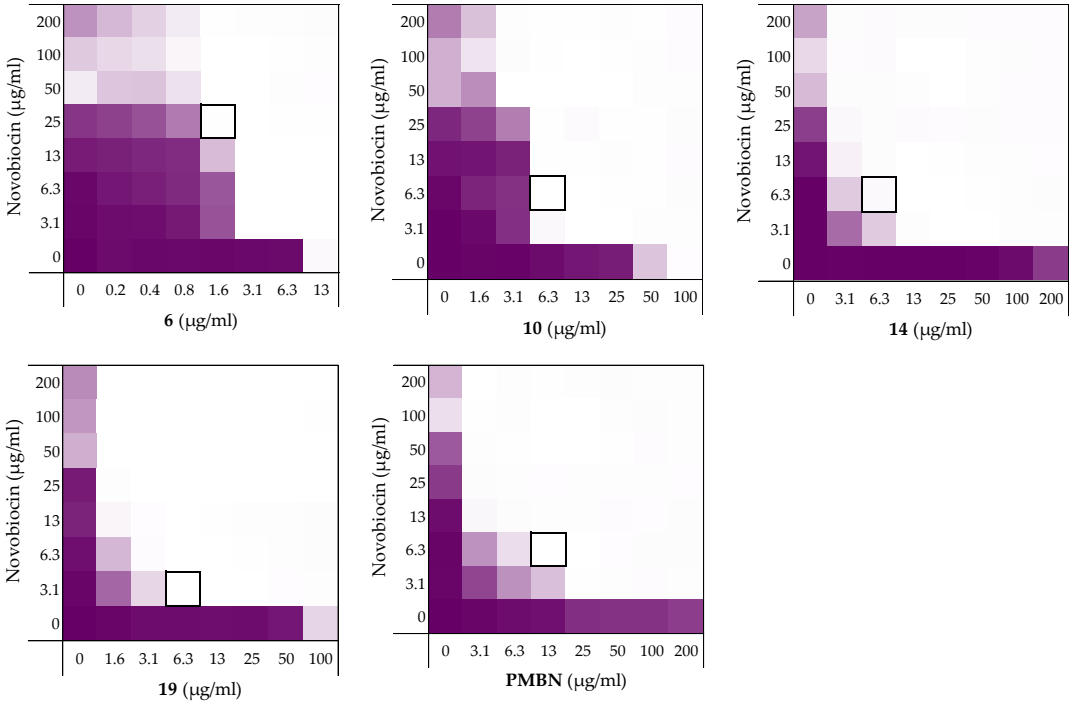

Figure S5. Checkerboard assays of the peptides **6**, **10**, **14**, **19** and PMBN in combination with novobiocin versus *E. coli* BW25113. OD600 values were measured using a plate reader and transformed to a gradient: purple represents growth, white represents no growth. In each case, the bounded box in the checkerboard assays indicates the minimal synergistic concentration (MSC) of compound and antibiotic resulting in the lowest FICI.

Table S5. Synergistic data of peptides **6**, **10**, **14**, **19** and PMBN of the checkerboard results for *E. coli* BW25113 with novobiocin displayed in Figure S5. All minimal inhibitory concentrations (MICs) and minimal synergistic concentrations (MSCs) are in µg/mL.

	$MIC_{peptide}$	$MSC_{peptide}$	MIC_{novo}	MSC_{novo}	FICI
6	12.5	1.563	>200	25	0.1875
10	100	6.25	>200	6.25	0.0781
14	>200	6.25	>200	6.25	0.0313
19	200	6.25	>200	3.125	0.0390
PMBN	>200	12.5	>200	6.25	0.0469

Checkerboard assays and FICI data against *E. coli* BW25113 with vancomycin

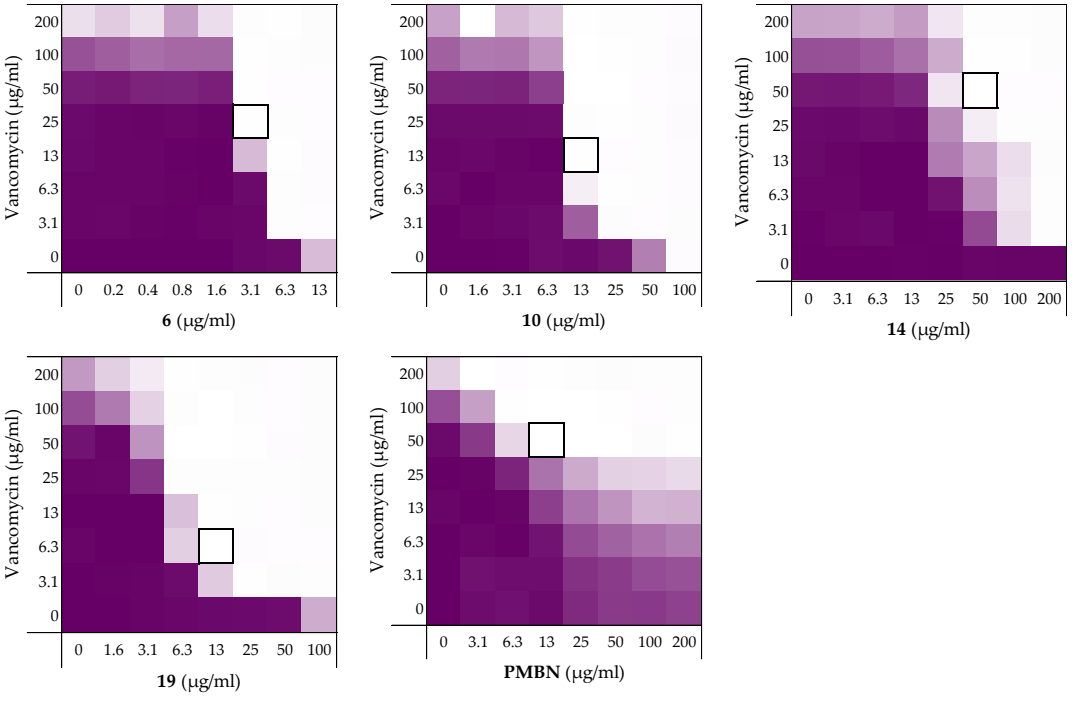

Figure S6. Checkerboard assays of the peptides **6**, **10**, **14**, **19** and PMBN in combination with vancomycin versus *E. coli* BW25113. OD600 values were measured using a plate reader and transformed to a gradient: purple represents growth, white represents no growth. In each case, the bounded box in the checkerboard assays indicates the minimal synergistic concentration (MSC) of compound and antibiotic resulting in the lowest FICI.

Table S6. Synergistic data of peptides **6**, **10**, **14**, **19** and PMBN of the checkerboard results for *E. coli* BW25113 with vancomycin displayed in Figure S6. All minimal inhibitory concentrations (MICs) and minimal synergistic concentrations (MSCs) are in µg/mL.

	$MIC_{peptide}$	$MSC_{peptide}$	MIC_{vanco}	MSC_{vanco}	FICI
6	25	3.125	>200	25	0.1875
10	100	12.5	>200	12.5	0.1563
14	>200	50	>200	50	0.2500
19	200	12.5	>200	6.25	0.0781
PMBN	>200	12.5	>200	50	0.1563

Checkerboard assays and FICI data against *E. coli* ATCC25922 with rifampicin

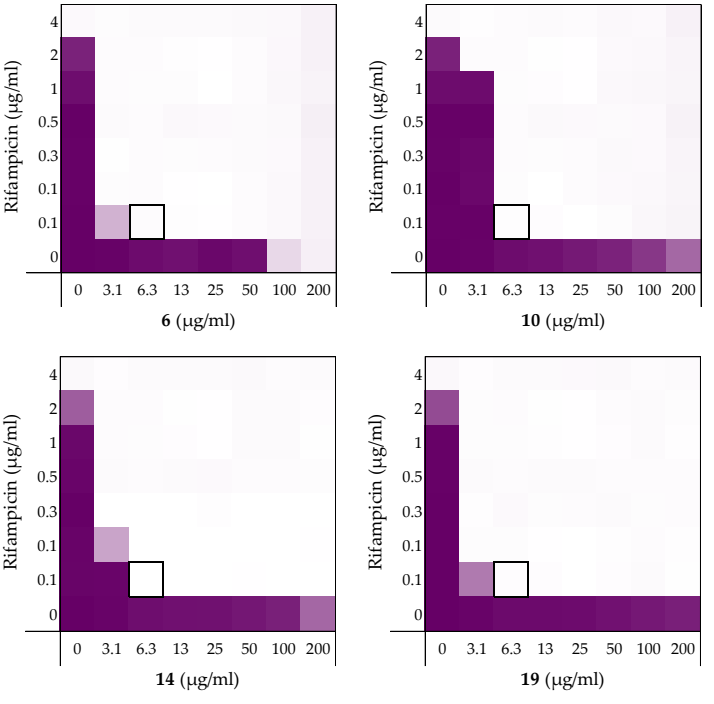

Figure S7. Checkerboard assays of the peptides **6**, **10**, **14**, and **19** in combination with rifampicin versus *E. coli* ATCC25922. OD600 values were measured using a plate reader and transformed to a gradient: purple represents growth, white represents no growth. In each case, the bounded box in the checkerboard assays indicates the minimal synergistic concentration (MSC) of compound and antibiotic resulting in the lowest FICI.

Table S7. Synergistic data of peptides **6**, **10**, **14**, and **19** of the checkerboard results for *E. coli* ATCC25922 with rifampicin displayed in Figure S7. All minimal inhibitory concentrations (MICs) and minimal synergistic concentrations (MSCs) are in µg/mL.

	$MIC_{peptide}$	$MSC_{peptide}$	MIC_{rif}	MSC_{rif}	FICI
6	200	6.25	4	0.063	0.0469
10	>200	6.25	4	0.063	0.0313
14	>200	6.25	4	0.063	0.0313
19	>200	6.25	4	0.063	0.0313

Checkerboard assays and FICI data against *E. coli* W3110 with rifampicin

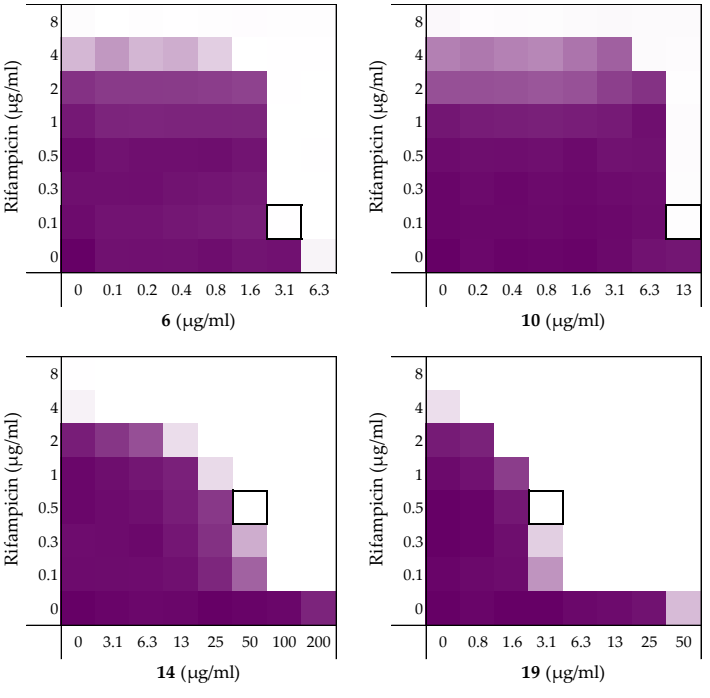

Figure S8. Checkerboard assays of the peptides **6**, **10**, **14**, and **19** in combination with rifampicin versus *E. coli* W3110. OD600 values were measured using a plate reader and transformed to a gradient: purple represents growth, white represents no growth. In each case, the bounded box in the checkerboard assays indicates the minimal synergistic concentration (MSC) of compound and antibiotic resulting in the lowest FICI.

Table S8. Synergistic data of peptides **6**, **10**, **14**, and **19** of the checkerboard results for *E. coli* W3110 with rifampicin displayed in Figure S8. All minimal inhibitory concentrations (MICs) and minimal synergistic concentrations (MSCs) are in µg/mL.

	$MIC_{peptide}$	$MSC_{peptide}$	MIC_{rif}	MSC_{rif}	FICI
6	6.25	3.125	8	0.125	>0.5[a]
10	25	12.5	8	0.125	>0.5[a]
14	>200	50	8	0.5	0.1875
19	100	3.125	8	0.5	0.0782

[a] Synergy is defined as FICI ≤0.5.[37]

Checkerboard assays and FICI data against *E. coli* mcr-1 with rifampicin

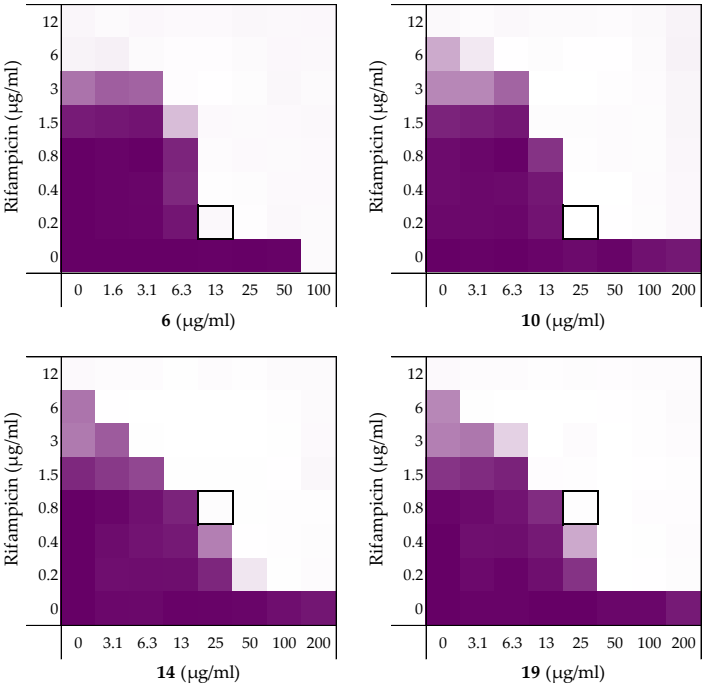

Figure S9. Checkerboard assays of the peptides **6**, **10**, **14**, and **19** in combination with rifampicin versus *E. coli* mcr-1. OD600 values were measured using a plate reader and transformed to a gradient: purple represents growth, white represents no growth. In each case, the bounded box in the checkerboard assays indicates the minimal synergistic concentration (MSC) of compound and antibiotic resulting in the lowest FICI.

Table S9. Synergistic data of peptides **6**, **10**, **14**, and **19** of the checkerboard results for *E. coli* mcr-1 with rifampicin displayed in Figure S9. All minimal inhibitory concentrations (MICs) and minimal synergistic concentrations (MSCs) are in μg/mL.

	$MIC_{peptide}$	$MSC_{peptide}$	MIC_{rif}	MSC_{rif}	FICI
6	100	12.5	12	0.188	0.1406
10	>200	25	12	0.188	0.0781
14	>200	25	12	0.75	0.1250
19	>200	25	12	0.75	0.1250

Checkerboard assays and FICI data against *E. coli* EQASmcr-1 with rifampicin

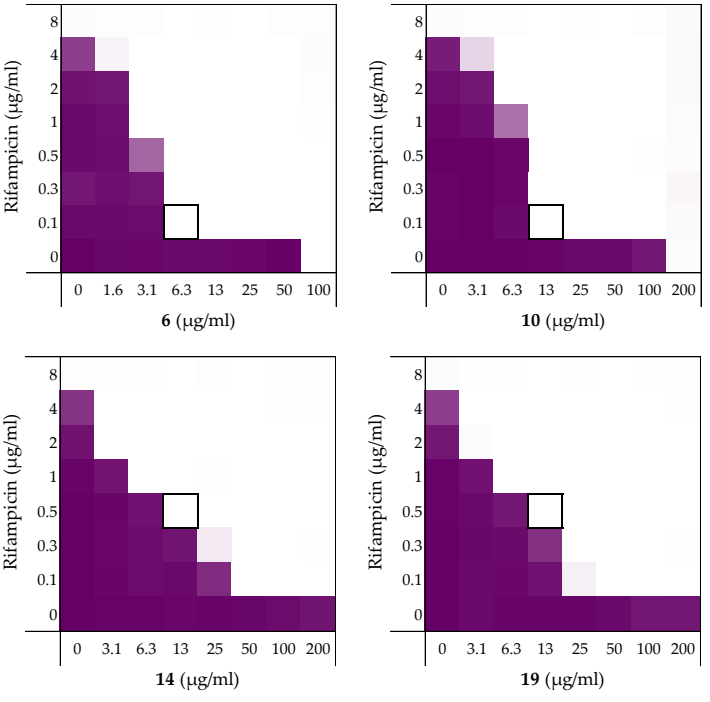

Figure S10. Checkerboard assays of the peptides **6**, **10**, **14**, and **19** in combination with rifampicin versus *E. coli* EQASmcr-1. OD600 values were measured using a plate reader and transformed to a gradient: purple represents growth, white represents no growth. In each case, the bounded box in the checkerboard assays indicates the minimal synergistic concentration (MSC) of compound and antibiotic resulting in the lowest FICI.

Table S10. Synergistic data of peptides **6**, **10**, **14**, and **19** of the checkerboard results for *E. coli* EQASmcr-1 with rifampicin displayed in Figure S10. All minimal inhibitory concentrations (MICs) and minimal synergistic concentrations (MSCs) are in µg/mL.

	$MIC_{peptide}$	$MSC_{peptide}$	MIC_{rif}	MSC_{rif}	FICI
6	100	6.25	8	0.125	0.0781
10	200	12.5	8	0.125	0.0781
14	>200	12.5	8	0.5	0.0938
19	>200	12.5	8	0.5	0.0938

Checkerboard assays and FICI data against *E. coli* EQASmcr-2 with rifampicin

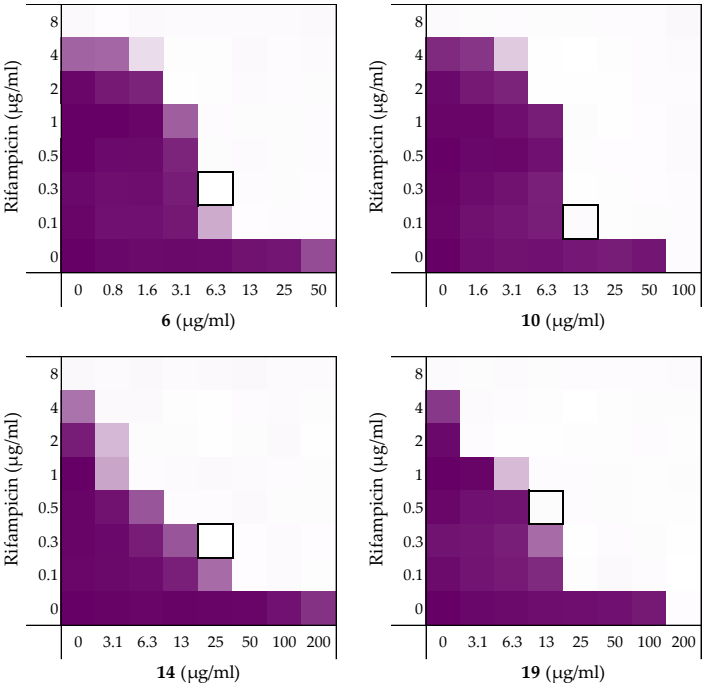

Figure S11. Checkerboard assays of the peptides **6**, **10**, **14**, and **19** in combination with rifampicin versus *E. coli* EQASmcr-2. OD600 values were measured using a plate reader and transformed to a gradient: purple represents growth, white represents no growth. In each case, the bounded box in the checkerboard assays indicates the minimal synergistic concentration (MSC) of compound and antibiotic resulting in the lowest FICI.

Table S11. Synergistic data of peptides **6**, **10**, **14**, and **19** of the checkerboard results for *E. coli* EQASmcr-2 with rifampicin displayed in Figure S11. All minimal inhibitory concentrations (MICs) and minimal synergistic concentrations (MSCs) are in µg/mL.

	$MIC_{peptide}$	$MSC_{peptide}$	MIC_{rif}	MSC_{rif}	FICI
6	100	6.25	8	0.25	0.0938
10	100	12.5	8	0.125	0.1406
14	>200	25	8	0.25	0.0938
19	200	12.5	8	0.5	0.1250

Checkerboard assays and FICI data against *E. coli* EQASmcr-3 with rifampicin

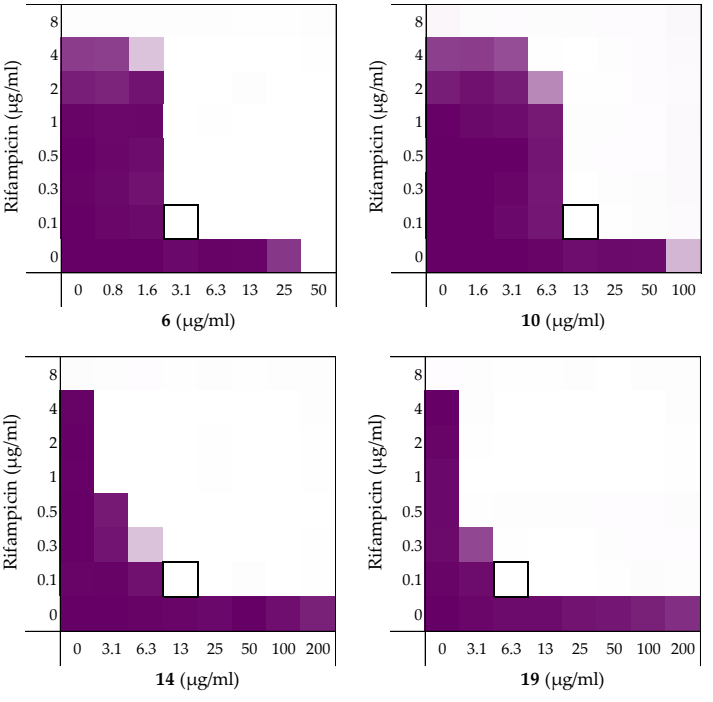

Figure S12. Checkerboard assays of the peptides **6**, **10**, **14**, and **19** in combination with rifampicin versus *E. coli* EQASmcr-3. OD600 values were measured using a plate reader and transformed to a gradient: purple represents growth, white represents no growth. In each case, the bounded box in the checkerboard assays indicates the minimal synergistic concentration (MSC) of compound and antibiotic resulting in the lowest FICI.

Table S12. Synergistic data of peptides **6**, **10**, **14**, and **19** of the checkerboard results for *E. coli* EQASmcr-3 with rifampicin displayed in Figure S12. All minimal inhibitory concentrations (MICs) and minimal synergistic concentrations (MSCs) are in µg/mL.

	$MIC_{peptide}$	$MSC_{peptide}$	MIC_{rif}	MSC_{rif}	FICI
6	50	3.125	8	0.125	0.0781
10	200	12.5	8	0.125	0.0781
14	>200	12.5	8	0.125	0.0469
19	>200	6.25	8	0.125	0.3125

Checkerboard assays and FICI data against *A. baumannii* **ATCC17978 with rifampicin**

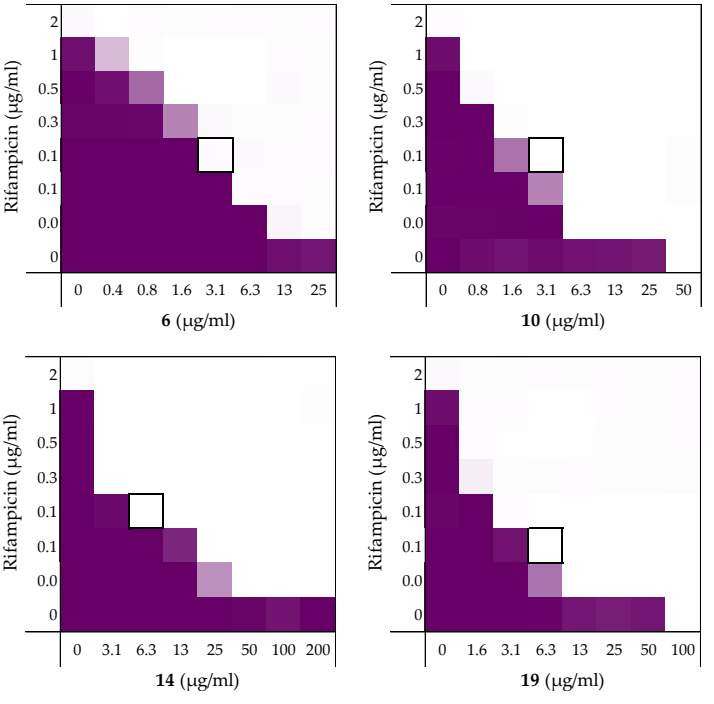

Figure S13. Checkerboard assays of the peptides **6**, **10**, **14**, and **19** in combination with rifampicin versus *A. baumannii* ATCC17978. OD600 values were measured using a plate reader and transformed to a gradient: purple represents growth, white represents no growth. In each case, the bounded box in the checkerboard assays indicates the minimal synergistic concentration (MSC) of compound and antibiotic resulting in the lowest FICI.

Table S13. Synergistic data of peptides **6**, **10**, **14**, and **19** of the checkerboard results for *A. baumannii* ATCC17978 with rifampicin displayed in Figure S13. All minimal inhibitory concentrations (MICs) and minimal synergistic concentrations (MSCs) are in µg/mL.

	$MIC_{peptide}$	$MSC_{peptide}$	MIC_{rif}	MSC_{rif}	FICI
6	50	3.125	2	0.125	0.1250
10	50	3.125	2	0.125	0.1250
14	>200	6.25	2	0.125	0.0781
19	100	6.25	2	0.063	0.0938

Checkerboard assays and FICI data against *K. pneumoniae* **ATCC13883 with rifampicin**

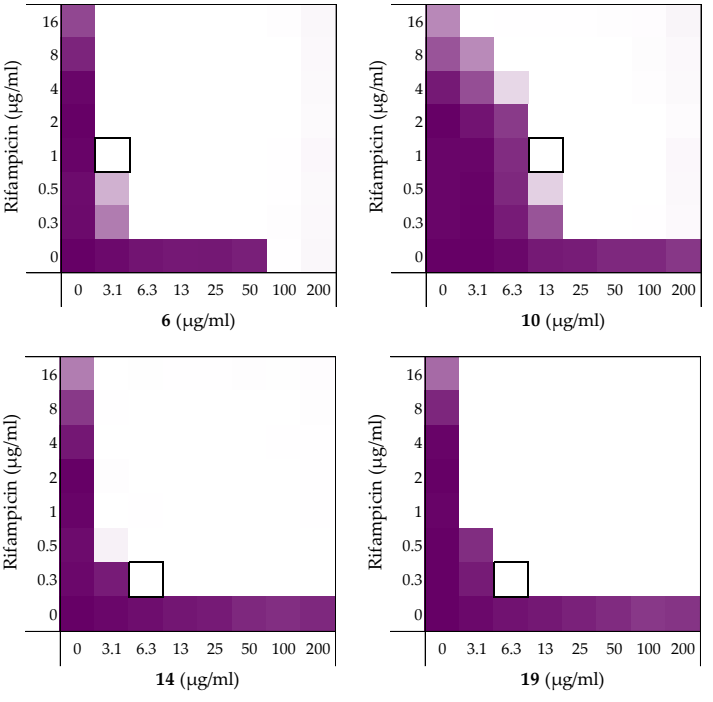

Figure S14. Checkerboard assays of the peptides **6**, **10**, **14**, and **19** in combination with rifampicin versus *K. pneumoniae* ATCC13883. OD600 values were measured using a plate reader and transformed to a gradient: purple represents growth, white represents no growth. In each case, the bounded box in the checkerboard assays indicates the minimal synergistic concentration (MSC) of compound and antibiotic resulting in the lowest FICI.

Table S14. Synergistic data of peptides **6**, **10**, **14**, and **19** of the checkerboard results for *K. pneumoniae* ATCC13883 with rifampicin displayed in Figure S14. All minimal inhibitory concentrations (MICs) and minimal synergistic concentrations (MSCs) are in µg/mL.

	$MIC_{peptide}$	$MSC_{peptide}$	MIC_{rif}	MSC_{rif}	FICI
6	100	3.125	32	1	0.0625
10	>200	12.5	32	1	0.0625
14	>200	6.25	32	0.25	0.0234
19	>200	6.25	32	0.25	0.0234

Checkerboard assays and FICI data against *P. aeruginosa* ATCC27853 with rifampicin

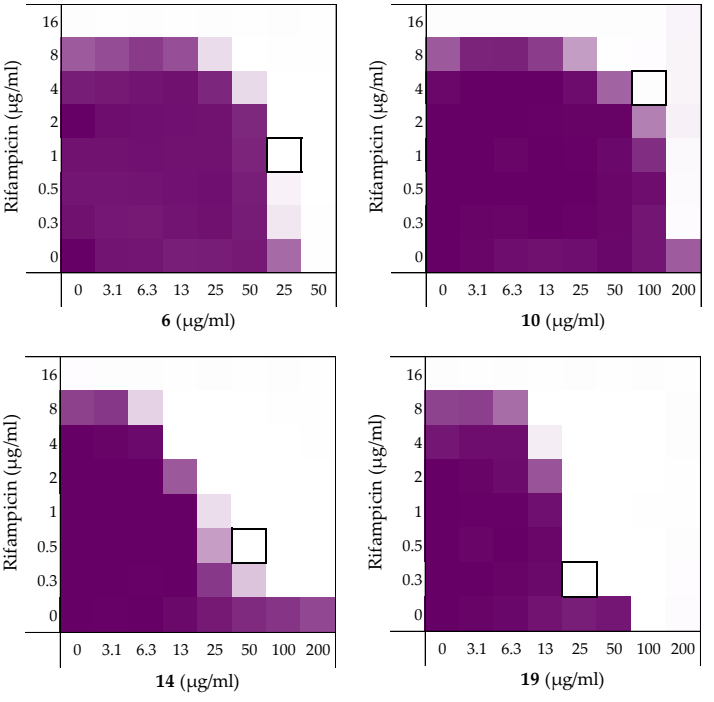

Figure S15. Checkerboard assays of the peptides **6**, **10**, **14**, and **19** in combination with rifampicin versus *P. aeruginosa* ATCC27853. OD600 values were measured using a plate reader and transformed to a gradient: purple represents growth, white represents no growth. In each case, the bounded box in the checkerboard assays indicates the minimal synergistic concentration (MSC) of compound and antibiotic resulting in the lowest FICI.

Table S15. Synergistic data of peptides **6**, **10**, **14**, and **19** of the checkerboard results for *P. aeruginosa* ATCC27853 with rifampicin displayed in Figure S15. All minimal inhibitory concentrations (MICs) and minimal synergistic concentrations (MSCs) are in µg/mL.

	$MIC_{peptide}$	$MSC_{peptide}$	MIC_{rif}	MSC_{rif}	FICI
6	50	25	16	1	>0.5 [a]
10	>200	100	16	4	0.2500
14	>200	50	16	0.5	0.1563
19	100	25	16	0.25	0.2656

[a] Synergy is defined as FICI ≤0.5.[37]

Membrane permeability assay using NPN

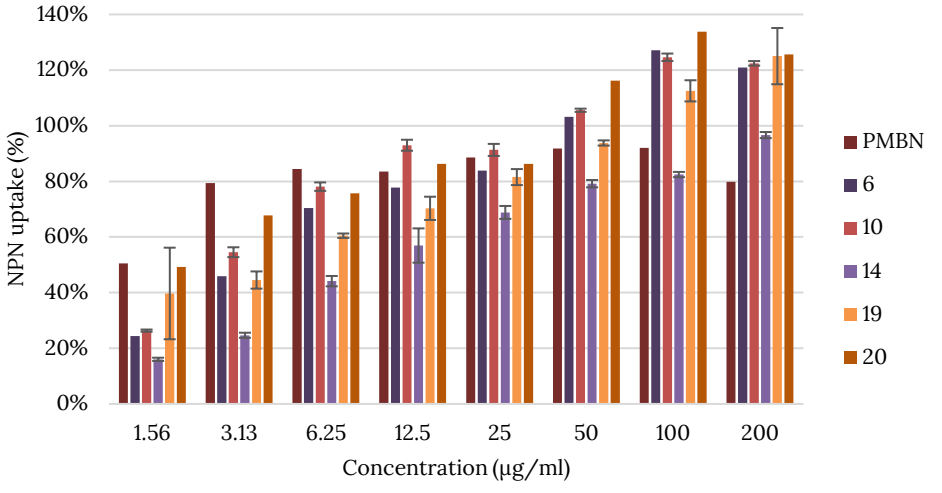

Figure S16. Outer membrane permeabilization assay of peptides **6**, **10**, **14**, **19**, **20**, and PMBN with *E. coli* BW25113 using N-phenyl-napthalen-1-amine (NPN) (at 0.01 mM) as fluorescent probe. The read-out was performed using a plate reader with λ_{ex} 355 nm and λ_{em} 420 nm. The NPN uptake values shown are relative to the uptake signal obtained upon treating the cells with 100 µg/mL colistin as previously reported.[48] Error bars represent the standard deviation based on n=3 technical replicates.

Peptide characterization and analysis

HRMS characterization

Table S16. Overview of the HRMS results obtained using a Shimadzu Nexera X2 UHPLC system with a Waters Acquity HSS C18 column (2.1 × 100 mm, 1.8 μm) at 30 °C and equipped with a diode array detector. This system was connected to a Shimadzu 9030 QTOF mass spectrometer (ESI ionisation) calibrated internally with Agilent's API-TOF reference mass solution kit (5.0 mM purine, 100.0 mM ammonium trifluoroacetate and 2.5 mM hexakis(1H,1H,3H-tetrafluoropropoxy)phosphazine) diluted to achieve a mass count of 10000.

	Peptide sequence	[M+H$^+$] calculated	[M+H$^+$] found
1	H_2N-VFRLKKWIQKVI-COOH	1557.9998	1557.9993
2	H_2N-HVFRLKKWIQKVIDQFGE-COOH	2271.2767	2271.2791
3	H_2N-FYTHVFRLKKWIQKVIDQFGE-COOH	2682.4561	2682.4579
4	H_2N-GKYGFYTHVFRLKKWIQKVIDQFGE-COOH	3087.6573	1544.3326[a]
5	Ac-VFRLKKWIQKVI-COOH	1600.0104	1600.0110
6	H_2N-VFRLKKWIQKVI-$CONH_2$	1557.0158	1557.0153
7	Ac-VFRLKKWIQKVI-$CONH_2$	1599.0263	1599.0259
8	H_2N-**A**FRLKKWIQKVI-$CONH_2$	1528.9845	1528.9753
9	H_2N-V**A**RLKKWIQKVI-$CONH_2$	1480.9845	1480.9846
10	H_2N-VF**A**LKKWIQKVI-$CONH_2$	1471.9518	1471.9523
11	H_2N-VFR**A**KKWIQKVI-$CONH_2$	1514.9688	1514.9685
12	H_2N-VFRL**A**KWIQKVI-$CONH_2$	1499.9579	1499.9580
13	H_2N-VFRLK**A**WIQKVI-$CONH_2$	1499.9579	1499.9578
14	H_2N-VFRLKK**A**IQKVI-$CONH_2$	1441.9736	1441.9736
15	H_2N-VFRLKKW**A**QKVI-$CONH_2$	1514.9688	1514.9696
16	H_2N-VFRLKKWI**A**KVI-$CONH_2$	1499.9943	1500.0008
17	H_2N-VFRLKKWIQ**A**VI-$CONH_2$	1499.9579	1499.9646
18	H_2N-VFRLKKWIQK**A**I-$CONH_2$	1528.9845	1528.9912
19	H_2N-VFRLKKWIQKV**A**-$CONH_2$	1514.9688	1514.9753
20	H_2N-vfrlkkwiqkvi-$CONH_2$	1557.0158	1557.0156
21	H_2N-IVKQIWKKLRFV-$CONH_2$	1557.0158	1557.0151
22	H_2N-ivkqiwkklrfv-$CONH_2$	1557.0158	1557.0222

[a] In this case only the $[M+2H]^{2+}$ was observed

References

(1) Freire-Moran, L.; Aronsson, B.; Manz, C.; Gyssens, I. C.; So, A. D.; Monnet, D. L.; Cars, O. Critical Shortage of New Antibiotics in Development against Multidrug-Resistant Bacteria—Time to React Is Now. *Drug Resistance Updates* **2011**, *14* (2), 118–124. https://doi.org/10.1016/j.drup.2011.02.003.

(2) Amann, S.; Neef, K.; Kohl, S. Antimicrobial Resistance (AMR). *Eur J Hosp Pharm* **2019**, *26* (3), 175–177. https://doi.org/10.1136/ejhpharm-2018-001820.

(3) Willyard, C. The Drug-Resistant Bacteria That Pose the Greatest Health Threats. *Nature* **2017**, *543* 7643), 15–15. https://doi.org/10.1038/nature.2017.21550.

(4) Nikaido, H. Molecular Basis of Bacterial Outer Membrane Permeability Revisited. *Microbiology and Molecular Biology Reviews* **2003**, *67* (4), 593–656. https://doi.org/10.1128/MMBR.67.4.593-656.2003.

(5) Silhavy, T. J.; Kahne, D.; Walker, S. The Bacterial Cell Envelope. *Cold Spring Harbor Perpectives in Biology* **2010**, 1–16. https://doi.org/10.1101/cshperspect.a000414.

(6) Vaara, M.; Vaara, T. Sensitization of Gram-Negative Bacteria to Antibiotics and Complement by a Nontoxic Oligopeptide. *Nature* **1983**, *303* (5917), 526–528. https://doi.org/10.1038/303526a0.

(7) Vaara, M. Agents That Increase the Permeability of the Outer Membrane. *Microbiol Rev* **1992**, *56* (3), 395–411.

(8) Rojas, E. R.; Billings, G.; Odermatt, P. D.; Auer, G. K.; Zhu, L.; Miguel, A.; Chang, F.; Weibel, D. B.; Theriot, J. A.; Huang, K. C. The Outer Membrane Is an Essential Load-Bearing Element in Gram-Negative Bacteria. *Nature* **2018**, *559* (7715), 617–621. https://doi.org/10.1038/s41586-018-0344-3.

(9) Kimura, Y.; Matsunaga, H.; Vaara, M. Polymyxin B Octapeptide and Polymyxin B Heptapeptide Are Potent Outer Membrane Permeability-Increasing Agents. *J Antibiot (Tokyo)* **1992**, *45* (5), 742–749. https://doi.org/10.7164/antibiotics.45.742.

(10) Lam, C.; Hildebrandt, J.; Schütze, E.; Wenzel, A. F. Membrane-Disorganizing Property of Polymyxin B Nonapeptide. *Journal of Antimicrobial Chemotherapy* **1986**, *18* (1), 9–15. https://doi.org/10.1093/jac/18.1.9.

(11) Viljanen, P.; Vaara, M. Susceptibility of Gram-Negative Bacteria to Polymyxin B Nonapeptide. *Antimicrobial Agents and Chemotherapy* **1984**, *25* (6), 701–705. https://doi.org/10.1128/AAC.25.6.701.

(12) Viljanen, P.; Koski, P.; Vaara, M. Effect of Small Cationic Leukocyte Peptides (Defensins) on the Permeability Barrier of the Outer Membrane. *Infect Immun* **1988**, *56* (9), 2324–2329.

(13) Tyrrell, J. M.; Aboklaish, A. F.; Walsh, T. R.; Vaara, T.; Vaara, M. The Polymyxin Derivative NAB739 Is Synergistic with Several Antibiotics against Polymyxin-Resistant Strains of Escherichia Coli, Klebsiella Pneumoniae and Acinetobacter Baumannii. *Peptides* **2019**, *112*, 149–153. https://doi.org/10.1016/j.peptides.2018.12.006.

(14) Vaara, M. Polymyxin Derivatives That Sensitize Gram-Negative Bacteria to Other Antibiotics. *Molecules* **2019**, *24* (2), 249. https://doi.org/10.3390/molecules24020249.

(15) FDA Approves New Antibacterial Drug to Treat Complicated Urinary Tract Infections as Part of Ongoing Efforts to Address Antimicrobial Resistance | FDA.

(16) Spero Therapeutics Highlights SPR741 Phase 1 and Preclinical Data at the 28th European Congress of Clinical Microbiology and Infectious Diseases | Spero Therapeutics, Inc.

(17) Vaara, M.; Siikanen, O.; Apajalahti, J.; Fox, J.; Frimodt-Møller, N.; He, H.; Poudyal, A.; Li, J.; Nation, R. L.; Vaara, T. A Novel Polymyxin Derivative That Lacks the Fatty Acid Tail and Carries Only Three Positive Charges Has Strong Synergism with Agents Excluded by the Intact Outer Membrane. *Antimicrobial Agents and Chemotherapy* **2010**, *54* (8), 3341–3346. https://doi.org/10.1128/AAC.01439-09.

(18) Kubesch, P.; Maass, G.; Tummler, B.; Boggs, J.; Luciano, L. Interaction of Polymyxin B Nonapeptide with Anionic Phospholipids. *Biochemistry* **1987**, *26* (8), 2139–2149. https://doi.org/10.1021/bi00382a012.

(19) Vaara, M.; Viljanen, P. Binding of Polymyxin B Nonapeptide to Gram-Negative Bacteria. *Antimicrobial Agents and Chemotherapy* **1985**, *27* (4), 548–554. https://doi.org/10.1128/AAC.27.4.548.

(20) Vaara, M. Polymyxin B Nonapeptide Complexes with Lipopolysaccharide. *FEMS Microbiology Letters* **1983**, *18* (1–2), 117–121. https://doi.org/10.1111/j.1574-6968.1983.tb00461.x.

(21) Peterson, A. A.; Hancock, R. E. W.; McGroarty, E. J. Binding of Polycationic Antibiotics and Polyamines to Lipopolysaccharides of Pseudomonas Aeruginosa. *Journal of Bacteriology* **1985**, *164* (3), 1256–1261. https://doi.org/10.1128/jb.164.3.1256-1261.1985.

(22) Cavaillon, J. M.; Adib-Conquy, M. Bench-to-Bedside Review: Endotoxin Tolerance as a Model of Leukocyte Reprogramming in Sepsis. *Critical Care* **2006**, *10* (5), 1–8. https://doi.org/10.1186/cc5055.

(23) Fenton, M. J.; Golenbock, D. T. LPS-Binding Proteins and Receptors. *Journal of Leukocyte Biology* **1998**, *64* (1), 25–32. https://doi.org/10.1002/jlb.64.1.25.

(24) Rosenfeld, Y.; Shai, Y. Lipopolysaccharide (Endotoxin)-Host Defense Antibacterial Peptides Interactions: Role in Bacterial Resistance and Prevention of Sepsis. *Biochimica et Biophysica Acta - Biomembranes* **2006**, *1758* (9), 1513–1522. https://doi.org/10.1016/j.bbamem.2006.05.017.

(25) Brandenburg, K.; Heinbockel, L.; Correa, W.; Lohner, K. Peptides with Dual Mode of Action: Killing Bacteria and Preventing Endotoxin-Induced Sepsis. *Biochimica et Biophysica Acta - Biomembranes* **2016**, *1858* (5), 971–979. https://doi.org/10.1016/j.bbamem.2016.01.011.

(26) Saravanan, R.; Holdbrook, D. A.; Petrlova, J.; Singh, S.; Berglund, N. A.; Choong, Y. K.; Kjellström, S.; Bond, P. J.; Malmsten, M.; Schmidtchen, A. Structural Basis for Endotoxin Neutralisation and Anti-Inflammatory Activity of Thrombin-Derived C-Terminal Peptides. *Nat Commun* **2018**, *9* (1), 2762. https://doi.org/10.1038/s41467-018-05242-0.

(27) Dong, N.; Li, X. R.; Xu, X. Y.; Lv, Y. F.; Li, Z. Y.; Shan, A. S.; Wang, J. L. Correction to: Characterization of Bactericidal Efficiency, Cell Selectivity, and Mechanism of Short Interspecific Hybrid Peptides (Amino Acids, (2018), 50, 3-4, (453-468), 10.1007/S00726-017-2531-1). *Amino Acids* **2018**, *50* (7), 967–967. https://doi.org/10.1007/s00726-018-2584-9.

(28) Jerala, R.; Porro, M. Endotoxin Neutralizing Peptides. *Current Topics in Medicinal Chemistry* **2005**, *4* (11), 1173–1184. https://doi.org/10.2174/1568026043388079.

(29) Kaconis, Y.; Kowalski, I.; Howe, J.; Brauser, A.; Richter, W.; Razquin-Olazarán, I.; Inĩgo-Pestaña, M.; Garidel, P.; Rössle, M.; De Tejada, G. M.; Gutsmann, T.; Brandenburg, K. Biophysical Mechanisms of Endotoxin Neutralization by Cationic Amphiphilic Peptides. *Biophysical Journal* **2011**, *100* (11), 2652–2661. https://doi.org/10.1016/j.bpj.2011.04.041.

(30) De Tejada, G. M.; Heinbockel, L.; Ferrer-Espada, R.; Heine, H.; Alexander, C.; Bárcena-Varela, S.; Goldmann, T.; Correa, W.; Wiesmüller, K. H.; Gisch, N.; Sánchez-Gómez, S.; Fukuoka, S.; Schürholz, T.; Gutsmann, T.; Brandenburg, K. Lipoproteins/Peptides Are Sepsis-Inducing Toxins from Bacteria That Can Be Neutralized by Synthetic Anti-Endotoxin Peptides. *Scientific Reports* **2015**, *5* (August), 1–15. https://doi.org/10.1038/srep14292.

(31) Stokes, J. M.; MacNair, C. R.; Ilyas, B.; French, S.; Côté, J.-P.; Bouwman, C.; Farha, M. A.; Sieron, A. O.; Whitfield, C.; Coombes, B. K.; Brown, E. D. Pentamidine Sensitizes Gram-Negative Pathogens to Antibiotics and Overcomes Acquired Colistin Resistance. *Nat Microbiol* **2017**, *2* (5), 1–8. https://doi.org/10.1038/nmicrobiol.2017.28.

(32) Hancock, R. E. Alterations in Outer Membrane Permeability. *Annu Rev Microbiol* **1984**, *38*, 237–264. https://doi.org/10.1146/annurev.mi.38.100184.001321.

(33) Li, Q.; Cebrián, R.; Montalbán-López, M.; Ren, H.; Wu, W.; Kuipers, O. P. Outer-Membrane-Acting Peptides and Lipid II-Targeting Antibiotics Cooperatively Kill Gram-Negative Pathogens. *Commun Biol* **2021**, *4* (1), 1–11. https://doi.org/10.1038/s42003-020-01511-1.

(34) Papareddy, P.; Rydengård, V.; Pasupuleti, M.; Walse, B.; Mörgelin, M.; Chalupka, A.; Malmsten, M.; Schmidtchen, A. Proteolysis of Human Thrombin Generates Novel Host Defense Peptides. *PLoS pathogens* **2010**, *6* (4). https://doi.org/10.1371/journal.ppat.1000857.

(35) Kasetty, G.; Papareddy, P.; Kalle, M.; Rydengård, V.; Mörgelin, M.; Albiger, B.; Malmsten, M.; Schmidtchen, A. Structure-Activity Studies and Therapeutic Potential of Host Defense Peptides of Human Thrombin. *Antimicrobial Agents and Chemotherapy* **2011**, *55* (6), 2880–2890. https://doi.org/10.1128/AAC.01515-10.

(36) Holdbrook, D. A.; Singh, S.; Choong, Y. K.; Petrlova, J.; Malmsten, M.; Bond, P. J.; Verma, N. K.; Schmidtchen, A.; Saravanan, R. Influence of PH on the Activity of Thrombin-Derived Antimicrobial Peptides. *Biochimica et Biophysica Acta - Biomembranes* **2018**, *1860* (11), 2374–2384. https://doi.org/10.1016/j.bbamem.2018.06.002.

(37) Odds, F. C. Synergy, Antagonism, and What the Chequerboard Puts between Them. *Journal of Antimicrobial Chemotherapy* **2003**, *52* (1), 1–1. https://doi.org/10.1093/jac/dkg301.

(38) Washington, J. A.; Wilson, W. R. Erythromycin: A Microbial and Clinical Perspective after 30 Years of Clinical Use (First of Two Parts). *Mayo Clinic Proceedings* **1985**, *60* (3), 189–203. https://doi.org/10.1016/S0025-6196(12)60219-5.

(39) Washington, J. A.; Wilson, W. R. Erythromycin: A Microbial and Clinical Perspective after 30 Years of Clinical Use (Second of Two Parts). *Mayo Clinic Proceedings* **1985**, *60* (4), 271–278. https://doi.org/10.1016/S0025-6196(12)60322-X.

(40) Farr, B.; Mandell, G. L. Rifampin. *Medical Clinics of North America* **1982**, *66* (1), 157–168. https://doi.org/10.1016/S0025-7125(16)31449-3.

(41) Furevi, A.; Ståhle, J.; Muheim, C.; Gkotzis, S.; Udekwu, K. I.; Daley, D. O.; Widmalm, G. Structural Analysis of the O-Antigen Polysaccharide from Escherichia Coli O188. *Carbohydrate Research* **2020**, *498* (2020), 108051–108051. https://doi.org/10.1016/j.carres.2020.108051.

(42) Uchida, K.; Mizushima, S. A Simple Method for Isolation of Lipopolysaccharides from Pseudomonas Aeruginosa and Some Other Bacterial Strains. *Agricultural and Biological Chemistry* **1987**, *51* (11), 3107–3114. https://doi.org/10.1080/00021369.1987.10868532.

(43) Ebbensgaard, A.; Mordhorst, H.; Aarestrup, F. M.; Hansen, E. B. The Role of Outer Membrane Proteins and Lipopolysaccharides for the Sensitivity of Escherichia Coli to Antimicrobial Peptides. *Frontiers in Microbiology* **2018**, *9* (SEP), 2153–2153. https://doi.org/10.3389/fmicb.2018.02153.

(44) Wang, Z.; Wang, J.; Ren, G.; Li, Y.; Wang, X. Influence of Core Oligosaccharide of Lipopolysaccharide to Outer Membrane Behavior of Escherichia Coli. *Marine Drugs* **2015**, *13* (6), 3325–3339. https://doi.org/10.3390/md13063325.

(45) Liu, Y. Y.; Wang, Y.; Walsh, T. R.; Yi, L. X.; Zhang, R.; Spencer, J.; Doi, Y.; Tian, G.; Dong, B.; Huang, X.; Yu, L. F.; Gu, D.; Ren, H.; Chen, X.; Lv, L.; He, D.; Zhou, H.; Liang, Z.; Liu, J. H.; Shen, J. Emergence of Plasmid-Mediated Colistin Resistance Mechanism MCR-1 in Animals and Human Beings in China: A Microbiological and Molecular Biological Study. *The Lancet Infectious Diseases* **2016**, *16* (2), 161–168. https://doi.org/10.1016/S1473-3099(15)00424-7.

(46) Nang, S. C.; Li, J.; Velkov, T. The Rise and Spread of Mcr Plasmid-Mediated Polymyxin Resistance. *Critical Reviews in Microbiology* **2019**, *45* (2), 131–161. https://doi.org/10.1080/1040841X.2018.1492902.

(47) Helander, I. M.; Mattila-Sandholm, T. Fluorometric Assessment of Gram-Negative Bacterial Permeabilization. *Journal of Applied Microbiology* **2000**, *88* (2), 213–219. https://doi.org/10.1046/j.1365-2672.2000.00971.x.

(48) MacNair, C. R.; Stokes, J. M.; Carfrae, L. A.; Fiebig-Comyn, A. A.; Coombes, B. K.; Mulvey, M. R.; Brown, E. D. Overcoming Mcr-1 Mediated Colistin Resistance with Colistin in Combination with Other Antibiotics. *Nat Commun* **2018**, *9* (1), 458. https://doi.org/10.1038/s41467-018-02875-z.

(49) Van Regenmortel, M. H. V.; Muller, S. D-Peptides as Immunogens and Diagnostic Reagents. *Current Opinion in Biotechnology* **1998**, *9* (4), 377–382. https://doi.org/10.1016/S0958-1669(98)80011-6.

(50) Singh, S.; Kalle, M.; Papareddy, P.; Schmidtchen, A.; Malmsten, M. Lipopolysaccharide Interactions of C-Terminal Peptides from Human Thrombin. *Biomacromolecules* **2013**, *14* (5), 1482–1492. https://doi.org/10.1021/bm400150c.

(51) Oliva, R.; Battista, F.; Cozzolino, S.; Notomista, E.; Winter, R.; Del Vecchio, P.; Petraccone, L. Encapsulating Properties of Sulfobutylether-β-Cyclodextrin toward a Thrombin-Derived Antimicrobial Peptide. *Journal of Thermal Analysis and Calorimetry* **2019**, *138* (5), 3249–3256. https://doi.org/10.1007/s10973-019-08609-7.

(52) Burdukiewicz, M.; Sidorczuk, K.; Rafacz, D.; Pietluch, F.; Chilimoniuk, J.; Rödiger, S.; Gagat, P. Proteomic Screening for Prediction and Design of Antimicrobial Peptides with AmpGram. *International Journal of Molecular Sciences* **2020**, *21* (12), 4310–4310. https://doi.org/10.3390/ijms21124310.

(53) Mura, M.; Wang, J.; Zhou, Y.; Pinna, M. The Effect of Amidation on the Behaviour of Antimicrobial Peptides. **2016**, 195–207. https://doi.org/10.1007/s00249-015-1094-x.

(54) Tsubery, H.; Ofek, I.; Cohen, S.; Fridkin, M. The Functional Association of Polymyxin B with Bacterial Lipopolysaccharide Is Stereospecific: Studies on Polymyxin B Nonapeptide. *Biochemistry* **2000**, *39* (39), 11837–11844. https://doi.org/10.1021/bi000386q.

(55) Jin, Y.; Mozsolits, H.; Hammer, J.; Zmuda, E.; Zhu, F.; Zhang, Y.; Aguilar, M. I.; Blazyk, J. Influence of Tryptophan on Lipid Binding of Linear Amphipathic Cationic Antimicrobial Peptides. *Biochemistry* **2003**, *42* (31), 9395–9405. https://doi.org/10.1021/bi034338s.

(56) Yau, W. M.; Wimley, W. C.; Gawrisch, K.; White, S. H. The Preference of Tryptophan for Membrane Interfaces. *Biochemistry* **1998**, *37* (42), 14713–14718. https://doi.org/10.1021/bi980809c.

(57) Wimley, W. C.; White, S. H. Experimentally Determined Hydrophobicity Scale for Proteins at Membrane Interfaces. *Nature Structural Biology* **1996**, *3* (10), 842–848. https://doi.org/10.1038/nsb1096-842.

(58) Strøm, M. B.; Haug, B. E.; Skar, M. L.; Stensen, W.; Stiberg, T.; Svendsen, J. S. The Pharmacophore of Short Cationic Antibacterial Peptides. *Journal of Medicinal Chemistry* **2003**, *46* (9), 1567–1570. https://doi.org/10.1021/jm0340039.

(59) Velkov, T.; Thompson, P. E.; Nation, R. L.; Li, J. Structure–Activity Relationships of Polymyxin Antibiotics. *J. Med. Chem.* **2010**, *53* (5), 1898–1916. https://doi.org/10.1021/jm900999h.

(60) Wang, J.; Chou, S.; Xu, L.; Zhu, X.; Dong, N.; Shan, A.; Chen, Z. High Specific Selectivity and Membrane-Active Mechanism of the Synthetic Centrosymmetric α-Helical Peptides with Gly-Gly Pairs. *Scientific Reports* **2015**, *5* (April), 1–19. https://doi.org/10.1038/srep15963.